Cabauw Experimental Results from the Project for Intercomparison of Land-Surface Parameterization Schemes

T. H. CHEN,[a] A. HENDERSON-SELLERS,[a] P. C. D. MILLY,[b] A. J. PITMAN,[a] A. C. M. BELJAARS,[c] J. POLCHER,[d]
F. ABRAMOPOULOS,[e] A. BOONE,[f] S. CHANG,[g] F. CHEN,[h] Y. DAI,[i] C. E. DESBOROUGH,[a] R. E. DICKINSON,[j]
L. DÜMENIL,[k] M. EK,[c] J. R. GARRATT,[l] N. GEDNEY,[m] Y. M. GUSEV,[n] J. KIM,[o] R. KOSTER,[p] E. A. KOWALCZYK,[l]
K. LAVAL,[d] J. LEAN,[q] D. LETTENMAIER,[r] X. LIANG,[s] J.-F. MAHFOUF,[t] H.-T. MENGELKAMP,[u] K. MITCHELL,[h]
O. N. NASONOVA,[n] J. NOILHAN,[v] A. ROBOCK,[w] C. ROSENZWEIG,[e] J. SCHAAKE,[x] C. A. SCHLOSSER,[w]
J.-P. SCHULZ,[k] Y. SHAO,[y] A. B. SHMAKIN,[z] D. L. VERSEGHY,[aa] P. WETZEL,[f] E. F. WOOD,[s] Y. XUE,[bb]
Z.-L. YANG,[j] AND Q. ZENG[i]

[a]*Climatic Impacts Centre, Macquarie University, Sydney, Australia*
[b]*U.S. Geological Survey and Geophysical Fluid Dynamics Laboratory/NOAA, Princeton, New Jersey*
[c]*Royal Netherlands Meteorological Institute, De Bilt, the Netherlands*
[d]*Laboratoire de Météorologie Dynamique du CNRS, Paris, France*
[e]*Science Systems and Applications Incorporated, New York City, New York*
[f]*Mesoscale Dynamics and Precipitation Branch, NASA/Goddard Space Flight Center, Greenbelt, Maryland*
[g]*Phillips Laboratory (PL/GPAB), Hanscom AFB, Massachusetts*
[h]*Development Division, National Centers for Environmental Prediction, NOAA, Camp Springs, Maryland*
[i]*Institute of Atmospheric Physics, Academy of Science, Beijing, People's Republic of China*
[j]*Institute of Atmospheric Physics, The University of Arizona, Tucson, Arizona*
[k]*Max-Planck-Institut für Meteorologie, Hamburg, Germany*
[l]*Division of Atmospheric Research, CSIRO, Aspendale, Victoria, Australia*
[m]*Meteorology Department, Reading University, Reading, United Kingdom*
[n]*Institute of Water Problems, Moscow, Russia*
[o]*Lawrence Livermore National Laboratory, Livermore, California*
[p]*Hydrological Sciences Branch, NASA/GSFC, Greenbelt, Maryland*
[q]*Hadley Centre for Climate Prediction and Research, Meteorological Office, Berkshire, United Kingdom*
[r]*Department of Civil Engineering, University of Washington, Seattle, Washington*
[s]*Department of Civil Engineering and Operations Research, Princeton University, Princeton, New Jersey*
[t]*ECMWF, Reading, United Kingdom*
[u]*Institute for Atmospheric Physics, GKSS–Research Center, Max-Planck-Strasse, Geesthacht, Germany*
[v]*Météo-France/CNRM, Toulouse, France*
[w]*Department of Meteorology, University of Maryland at College Park, College Park, Maryland*
[x]*Office of Hydrology, NWS/NOAA, Silver Spring, Maryland*
[y]*Centre for Advanced Numerical Computation in Engineering and Science, University of New South Wales, Sydney, Australia*
[z]*Institute of Geography, Moscow, Russia*
[aa]*Climate Research Branch, Atmospheric Environment Service, Downsview, Ontario, Canada*
[bb]*Centre for Ocean–Land–Atmosphere Studies, Calverton, Maryland*

ABSTRACT

In the Project for Intercomparison of Land-Surface Parameterization Schemes phase 2a experiment, meteo-rological data for the year 1987 from Cabauw, the Netherlands, were used as inputs to 23 land-surface flux schemes designed for use in climate and weather models. Schemes were evaluated by comparing their outputs with long-term measurements of surface sensible heat fluxes into the atmosphere and the ground, and of upward longwave radiation and total net radiative fluxes, and also comparing them with latent heat fluxes derived from a surface energy balance. Tuning of schemes by use of the observed flux data was not permitted. On an annual basis, the predicted surface radiative temperature exhibits a range of 2 K across schemes, consistent with the range of about 10 W m^{-2} in predicted surface net radiation. Most modeled values of monthly net radiation differ from the observations by less than the estimated maximum monthly observational error (± 10 W m^{-2}). However, modeled radiative surface temperature appears to have a systematic positive bias in most schemes; this might be explained by an error in assumed emissivity and by models' neglect of canopy thermal heterogeneity. Annual means of sensible and latent heat fluxes, into which net radiation is partitioned, have ranges across schemes of

Corresponding author address: Dr. Tian Hong Chen, Australian Oceanographic Data Centre, Maritime Headquarters, Potts Point, NSW 2001, Australia.
E-mail: tian@aodc.gov.au

30 W m^{-2} and 25 W m^{-2}, respectively. Annual totals of evapotranspiration and runoff, into which the precipitation is partitioned, both have ranges of 315 mm. These ranges in annual heat and water fluxes were approximately halved upon exclusion of the three schemes that have no stomatal resistance under non-water-stressed conditions. Many schemes tend to underestimate latent heat flux and overestimate sensible heat flux in summer, with a reverse tendency in winter. For six schemes, root-mean-square deviations of predictions from monthly observations are less than the estimated upper bounds on observation errors (5 W m^{-2} for sensible heat flux and 10 W m^{-2} for latent heat flux). Actual runoff at the site is believed to be dominated by vertical drainage to groundwater, but several schemes produced significant amounts of runoff as overland flow or interflow. There is a range across schemes of 184 mm (40% of total pore volume) in the simulated annual mean root-zone soil moisture. Unfortunately, no measurements of soil moisture were available for model evaluation. A theoretical analysis suggested that differences in boundary conditions used in various schemes are not sufficient to explain the large variance in soil moisture. However, many of the extreme values of soil moisture could be explained in terms of the particulars of experimental setup or excessive evapotranspiration.

---

1. Introduction

Project for Intercomparison of Land-Surface Parameterization Schemes (PILPS) is a World Climate Research Programme project operating under the auspices of the Global Energy and Water Cycle Experiment and the Working Group on Numerical Experimentation. Its goal is to improve understanding of the parameterization of interactions between the atmosphere and the continental surface in climate and weather forecast models. Since its establishment in 1992, PILPS has been responsible for a number of complementary sensitivity studies. In phase 1 of the project (Pitman et al. 1993), land-surface schemes were compared off-line using atmospheric forcing generated from a general circulation model, thereby preventing feedbacks between the atmosphere and the surface. Phase 2a, described in this paper, was again off-line, but observed point data from Cabauw, the Netherlands (51°58′N, 4°56′E), were used as the atmospheric forcing. Furthermore, observed flux data were available for evaluation of the performance of the schemes. The phase 2a experiment was the first one in which observational data were used in PILPS (Henderson-Sellers et al. 1995), and the aim was to determine how well individual land-surface schemes could reproduce a set of flux measurements at the Cabauw site taken coincidentally with the measurements of the atmospheric forcing.

Twenty-three land-surface schemes (Tables 1 and 2) participated in the PILPS phase 2a experiment. The focus of this study will be on a community-wide intercomparison among schemes, rather than on detailed analysis of individuals. The presentation of the experimental results is organized as follows. The observational data will be described in section 2. The experimental design and the underlying philosophy will be discussed in section 3, and the experimental results will be investigated in section 4. Finally, concluding remarks will be given in section 5. An appendix contains details of the Cabauw site characteristics and parameter setup.

2. Cabauw observational data

Rigorous testing of land-surface schemes requires accurate and contemporaneous observations of the input variables (henceforth "atmospheric forcing," which includes downward shortwave and longwave radiation, precipitation, surface atmospheric pressure, and near-surface air humidity, temperature, and wind speed), prognostic variables (surface temperatures and water stores), and output variables (net shortwave and longwave radiation, latent heat flux, sensible heat flux, ground heat flux, evapotranspiration, and runoff) of the schemes. Due to the importance of seasonal storage in the soil for water balance, and because of the large systematic changes in water and energy balances through the year, it is preferred to have at least 1 year of data. Although no available dataset was ideal for PILPS, several sets were sufficiently comprehensive to warrant consideration.

The Cabauw dataset was chosen for the PILPS phase 2a experiment for three reasons. First, it was planned within the PILPS framework to test land-surface schemes with different datasets representative of different land-surface conditions—Cabauw was a useful case study for midlatitude homogeneous grassland. Second, at Cabauw, deep soil is saturated throughout the year and evapotranspiration is seldom limited by water supply; this facilitates analysis of model outputs under the non-water-stressed condition, which is an important limiting case. It was anticipated that these two features of the Cabauw site might obviate some causes of the divergence among numerical simulations: the variability in water-storage time constants across schemes (Yang et al. 1995) and the variability in root-zone soil moisture across schemes (Shao et al. 1994). At the same time, of course, the rarity of water stress implies that the Cabauw data do not provide a good test of the models' ability to function when the water supply is limited. Finally, the Cabauw data include 1 full year of surface latent heat and sensible heat fluxes, providing a basis for testing model performance in terms of seasonal variation; many of the other available datasets, such as the Hydrological Atmospheric Pilot Experiment–Modélisation du Bilan Hydrique (Goutorbe and Tarrieu 1991), have these fluxes only for limited periods of time.

The Cabauw site consists mainly of short grass divided by narrow ditches. The climate in the area is characterized as "moderate maritime," with a prevailing

TABLE 1. List of land-surface schemes participating in PILPS phase 2a and some basic information about them.

Model	Contact	Number of layers for				Time step	Spinup time	Major purpose	Philosophy for			Reference
		C[a]	T[b]	S[c]	R[d]				C[a]	T[b]	S[c]	
BASE	C.E. Desborough A.J. Pitman	1	3	3	3	20 min	5 yr	GCM	Aerodynamic	Heat diffusion	Philip–de Vries	—
BATS	R.E. Dickinson Z.-L. Yang	1	2	3	2	30 min	3 yr	GCM	Penman–Monteith	Force–restore	Darcy's law	Dickinson et al. (1986, 1993)
BUCK	C.A. Schlosser	0	1	1	1	30 min	1 yr	GCM	Implicit	Heat balance	Bucket[e]	Manabe (1969)
CAPS	A. Robock S. Change M. Ek	1	3	3	2	30 min	1 yr	GCM	Penman–Monteith	Heat diffusion	Darcy's law	Robock et al. (1995) Mahrt and Pan (1984) Pan and Mahrt (1987)
CAPSLLNL	J. Kim	1	2	3	1	5 min	10 yr	GCM mesoscale	Penman–Monteith	Heat diffusion	Diffusion	Mahrt and Pan (1984) Kim and Ek (1995)
CAPSNMC	K. Mitchell F. Chen	1	3	3	2	30 min	3 yr	GCM mesoscale	Penman–Monteith	Heat diffusion	Darcy's law	Mahrt and Pan (1984) Pan and Mahrt (1987) Chen et al. (1996)
CLASS	D. Verseghy	1	3	3	3	30 min	3 yr	GCM	Penman–Monteith	Heat diffusion	Darcy's law	Verseghy (1991) Verseghy et al. (1993)
CSIRO9	E.A. Kowalczyk J.R. Garratt	1	3	2	1	30 min	2 yr	GCM	Aerodynamic	Heat diffusion	Force–restore	Kowalczyk et al. (1991)
ECHAM	L. Dümenil J.-P. Schulz	1	5	1	1	30 min	5 yr	GCM	Aerodynamic	Heat diffusion	Bucket[e]	Dümenil and Todini (1992)
GISS	F. Abramopoulos C. Rosenzweig	1	6	6	6	30 min	13 yr	GCM	Aerodynamic	Heat diffusion	Darcy's law	Abramopoulos et al. (1988) Rosenzweig and Abramopoulos (1991)
IAP94	Q. Zeng Y. Dai	1	3	3	2	60 min	60 yr	GCM	Penman–Monteith	Heat diffusion	Darcy's law	—
ISBA	J. Noilhan J.-F. Mahfouf	1	2	2	1	5 min	1 yr	GCM mesoscale	Aerodynamic	Force–restore	Force–restore	Noilhan and Planton (1989)
MOSAIC	R. Koster	1	2	3	2	5 min	6 yr	GCM	Penman–Monteith	Force–restore	Darcy's law	Koster and Suarez (1992)
PLACE	P. Wetzel A. Boone	1	7	50	2	30 min	3 yr	Flexible	Aerodynamic	Heat diffusion	Darcy's law	Wetzel and Boone (1995)
SECHIBA2	J. Polcher K. Laval	1	7	2	1	30 min	2 yr	GCM	Aerodynamic	Heat diffusion	Choisnel	Ducoudre et al. (1993)
SEWAB	H.-T. Mengelkamp	1	6	6	1	10–30 sec	3 yr	Mesoscale	Aerodynamic	Heat diffusion	Diffusion	—
SPONSOR	A.B. Shmakin	1	1	2	2	24 hr	3 yr	GCM	Aerodynamic	Energy balance	Bucket[e]	Shmakin et al. (1993)
SSiB	Y. Xue C.A. Schlosser	1	2	3	1	30 min	2 yr	GCM mesoscale	Penman–Monteith	Force–restore	Diffusion	Xue et al. (1991)
SWAP	Y.M. Gusev O. N. Nasonova	1	2	1	1	24 hr	2 yr	Mesoscale	Aerodynamic	Heat diffusion	Bucket[e]	—
SWB	J. Schaake V. Koren	0	3	2	2	30 min	3 yr	Mesoscale		Heat diffusion	Bucket[e]	Schaake et al. (1995)
UGAMP	N. Gedney	1	3	3	2	30 min	14 yr	GCM	Penman–Monteith	Heat diffusion	Darcy's law	—
UKMO	J. Lean	1	4	4	4	30 min	1 yr	GCM	Penman–Monteith	Heat diffusion	Darcy's law	Warrilow et al. (1986) Gregory and Smith (1994)
VIC-3L	X. Liang E. Wood D. Lettenmaier	1	2	3	2	60 min	2 yr	GCM mesoscale	Penman–Monteith	Heat diffusion capacity and more	Variable infiltration	Liange et al. (1994) Liang et al. (1996)

[a] Canopy.
[b] Soil temperature.
[c] Soil moisture.
[d] Roots.
[e] Bucket plus variation.

TABLE 2. Explanations of scheme acronyms.

Acronym	Explanation
BASE	Best Approximation of Surface Exchanges
BATS	Biosphere Atmosphere Transfer Scheme
BUCK	Bucket
CAPS	Coupled Atmosphere–Plant Soil model
CAPSLLNL	Coupled Atmosphere–Plant Soil model, Lawrence Livermore National Laboratory version
CAPSNMC	Coupled Atmosphere–Plant Soil model, National Meteorological Center (currently known as the National Centers for Environmental Prediction) version
CLASS	Canadian Land Surface Scheme
CSIRO9	CSIRO Soil-Canopy Scheme, nine-level GCM version
ECHAM	Land Surface Scheme of the ECHAM General Circulation Model
GISS	GISS Ground Hydrology Model
IAP94	Institute of Atmospheric Physics Land Surface Physical Processes Model for Atmospheric General Circulation Model, version 1994
ISBA	Interaction Soil Biosphere Atmosphere
MOSAIC	Mosaic
PLACE	Parameterization for Land–Atmosphere–Cloud Exchange
SECHIBA2	Schematisation des Echanges Hydriques Interface Biosphere–Atmosphere, version 2
SEWAB	Surface Energy and Water Balance scheme
SPONSOR	Semi-distributed Parameterization Scheme of the Orography-Induced Macrohydrology
SSiB	Simplified Simple Biosphere Model
SWAP	Soil Water–Atmosphere–Plant
SWB	Simple Water Balance Model
UGAMP	University Global Atmospheric Modelling Program
UKMO	The U.K. Meteorological Office Land Surface Scheme
VIC-3L	Three-Layer Variable Infiltration Capacity Scheme

FIG. 1. Cabauw 1987 monthly averaged meteorological data for the PILPS phase 2a experiment.

westerly. Up to a distance of about 200 m from the measurement site, there is no obstacle or perturbation of any importance; farther away, some scattered trees and houses are found for most wind directions. For easterly winds, the flow is perturbed by trees, orchards, and a village (Beljaars and Holtslag 1991).

The Cabauw data, provided by the Royal Netherlands Meteorological Institute, were based on a semioperational measurement program with a high level of quality control. Full details can be found in Driedonks et al. (1978), Monna and Van der Vliet (1987), and Beljaars and Bosveld (1997). The Cabauw data used in the PILPS phase 2a experiment cover the entire year of 1987. All components of the atmospheric forcing were included for input to the land-surface schemes. For evaluation of scheme outputs, energy-flux data including sensible and latent heat fluxes, net radiation, upward longwave radiation, and ground heat flux were available. The sensible and latent heat fluxes were not measured directly. Rather, the former was derived from temperature and wind profiles based on a modified flux-profile relationship, while the latter was derived as a residual of the surface energy balance (Beljaars 1982). When any of the measurements for the energy-flux variables listed
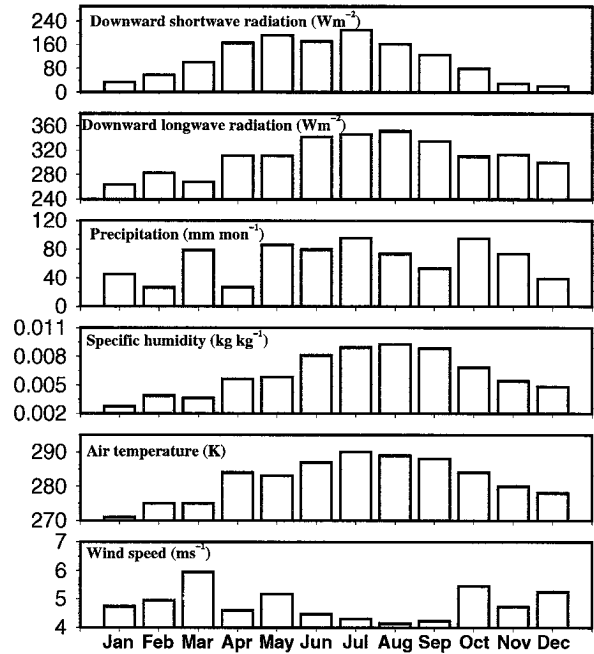
above were not available, data were derived from a parameterization scheme that has been calibrated locally and tested extensively against observed data (Holtslag and Van Ulden 1983). Both the forcing data and the energy fluxes for model evaluation were made available on a 30-min interval for 1 yr.

It needs to be mentioned that there are two versions of the Cabauw data. The forcing variables of the PILPS phase 2a experiment have been derived from version 1 (Beljaars and Viterbo 1994), but the energy fluxes for model evaluation have been derived from version 2 (Beljaars and Bosveld 1997); the latter included bias corrections to the former, which was initiated through the PILPS phase 2a experiment. As a result, there are some minor inconsistencies between the forcing data and the flux data for model evaluation. Tests on two schemes (BASE and CAPS) have shown that the inconsistencies have only limited impact on the model simulations. (For example, the differences between simulated annual mean sensible and latent heat fluxes using the two versions of forcing data are, respectively, 1.5 W m^{-2} and 0.5 W m^{-2} for BASE, and 1.6 W m^{-2} and 0.1 W m^{-2} for CAPS. Corresponding root-mean-square differences in monthly sensible and latent heat fluxes are 1.8 W m^{-2} and 0.9 W m^{-2} for BASE, and 2.2 and 1.1 W m^{-2} for CAPS.)

Figure 1 shows the monthly averaged meteorological observations. The observation height for the air temperature, wind, and specific humidity is 20 m. As shown, the annual cycles of radiation, specific humidity, and air temperature are in phase, but 180° out of phase with wind speed. The annual total precipitation is 776 mm,

10% above the climatological mean, and the annual mean air temperature is 282 K, 0.5 K below the climatological mean, indicating that 1987 was slightly wetter and cooler than average at Cabauw.

Estimation of the accuracy of the observed data is an important issue. There are a number of sources of error in the Cabauw data: the measurements themselves, the algorithm used to derive the sensible heat flux from measured variables, the substitution of data from a nearby synoptic station (De Bilt, 30 km away) for measurement gaps (due to instrument failure or data transmission problems), and errors in the parameterization scheme used to synthesize the missing energy fluxes for model evaluation. Beljaars and Bosveld (1997) have assessed the quality of the Cabauw dataset. They suggested that precipitation (the most difficult observation among the meteorological forcing variables) is possibly underestimated by 2%–11%, depending on wind. By exploiting the redundancy in observations and by comparing simulated data and observations when both are available, they subjectively estimated the range of error on monthly averages to be ± 5 W m^{-2} for sensible heat flux, ± 10 W m^{-2} for both latent heat flux and net radiation, and ± 1 W m^{-2} for ground heat flux at the surface. The ranges of observation error quoted here pertain to the maximum monthly mean differences between methods. In the evaluation of models, departures of model outputs from observations were considered significant if they fell outside these ranges.

Another discrepancy between simulations and observations is one of scale. This problem has not been tackled here—the assumption is made that PILPS's simulations are comparable with point observations. This assumption is justified, in part, by a survey distributed in 1992, in reply to which many modelers asserted that their land-surface schemes were independent of scale (Henderson-Sellers and Brown 1992). However, it is recognized that the scale issue could be the cause of some (perhaps many) of the discrepancies reported in this paper. Additionally, the approximation was made that 1987 was an equilibrium year (with identical initial and final states). The error induced by this approximation is expected to be limited in a very wet (and, presumably, short memory) system, such as the Cabauw site.

3. Design of numerical experiment

In accordance with the assumption that 1987 was an equilibrium year, each scheme was run using the observed 1987 forcing and repeated a sufficient number of times for the scheme to reach a dynamic equilibrium (defined below). For a lower boundary condition on water transfer, it was specified that a water table was present at 1-m depth. (This information was not used by all schemes, as discussed in a later section.) Deep vertical heat flux was taken to be negligible in all schemes. All schemes were initialized by saturating all liquid water stores and setting all temperatures to 279 K.

Equilibrium was defined as being the first occasion on which the January mean values of surface radiative temperature, latent and sensible heat fluxes, and root-zone soil moisture did not change by more than 0.01 K, 0.1 W m^{-2}, and 0.1 mm, respectively, from year N to year $N + 1$; the equilibration time was then N years. Actual spinup time n ($\geq N$) allowed by individual schemes is given in Table 1.

All land-surface schemes in the phase 2a experiment require virtually identical forcing variables, but their requirements for input parameters characterizing the land-surface differ in several respects (Polcher et al. 1996). For example, soil-water storage and release may be treated in one scheme using concepts of water potential and hydraulic conductivity, but in another scheme using the simpler concept of a lumped storage reservoir. The need to ensure consistency in the assignment of parameters (e.g., leaf area index, soil depth, albedo, and surface roughness) across schemes is a fundamental and continuing challenge in PILPS. The general approach taken was to describe the site physically in as much detail as possible and to assign parameters based on that physical description. In many cases, the detailed description was derived not from site-specific estimates, but from preexisting vegetation- and soil-dependent parameter tables in the more detailed land-surface schemes. Some details of the Cabauw site characteristics and parameter setup are given in the appendix.

It was required that no use of the observed data be made to tune any particular model. This was ensured by keeping the Cabauw flux data unreleased until experimental results from all experiment participants were submitted. However, the experiment outputs from different schemes were circulated among the participants at various stages, allowing modelers to identify mistakes in the specification of parameters and/or problems (e.g., model coding, underlying model philosophy, or structure) with schemes. Indeed, an important aspect of PILPS is that individual participants can improve their schemes during and following the process of intercomparison. The participants were allowed to correct these problems and resubmit their results, with a brief statement of the reasons for any change from their original runs. In addition, late submission of results (after the first circulation of results) was accepted. It cannot be excluded at this point that some information about the observed data and/or an earlier version of the figures shown in this paper were available to the participants. There are 6 schemes (BASE, ECHAM, GISS, PLACE, SPONSOR, and VIC-3L) from which experiment results have been updated since the first circulation and 2 (CAPSLLNL and IAP94) from which only one version of results was submitted, but after the first circulation.

Analyses of previous PILPS experiments revealed that differences among simulated variables, including latent and sensible heat fluxes, are affected by such com-

plications as differing interpretations of instructions and failures of outputs to satisfy energy balances (Milly et al. 1995; Henderson-Sellers et al. 1995; Love and Henderson-Sellers 1995). In phase 2a, it was required that all results must satisfy a series of tests before being considered in the analysis. For example, outputs from all schemes were checked to ensure the conservation of energy and water over the equilibrium year within the combined control volume of the soil root zone and the vegetation. Annual means of energy and water fluxes all obeyed

$$|R_n - LE - H| < 3 \text{ W m}^{-2}, \quad (1)$$

where R_n is net radiation, LE is latent heat flux, and H is sensible heat flux, and

$$|P - E - Y| < 3 \text{ mm}, \quad (2)$$

where P is precipitation, E is evapotranspiration, and Y is runoff. Runoff here is defined as the total liquid water loss from the root-zone–vegetation system by overland flow, lateral subsurface flow in the root zone, and downward flux across the bottom of the root zone; the last of these terms may be negative because of the presence of the water table. Ground heat flux is not included in (1) since its annual mean should be zero for the equilibrium year (the annual mean observed ground heat flux is 0.5 W m^{-2}). The latent heat of solid–liquid phase changes does not appear in (1) because of the small value (<1 W m^{-2}) of the associated terms. The same holds for the sensible heat transported by water entering and leaving the control volume.

4. Results from the Cabauw control simulations

In the PILPS phase 2a experiment, the required output results include a full year of daily mean values and 10 days (10–19 September) of individual model time step values. The analysis here will mainly be focused on energy and water budgets and their linkage, using annual mean, seasonal (monthly), and diurnal variations. To reconstruct a typical diurnal cycle, time step outputs have been averaged across the 10 days. Four schemes did not resolve the diurnal cycle, either because they used a 24-h time step (SPONSOR and SWAP) or because they employed forcing that was filtered to remove the diurnal cycle (BUCK and CAPSLLNL). These 4 schemes are excluded from the plots of diurnal variations. Three simple statistics to be used throughout this section are defined as follows: $M = 1/m \sum_{i=1}^{m} x_i$, STD $= \sqrt{1/m \sum_{i=1}^{m} (x_i - M)^2}$, and $D_i = x_i - M$, where i is a scheme index, m is the number of schemes (23), x is any output variable, M is its mean across schemes, STD is its standard deviation across schemes, and D_i is its deviation in scheme i from the mean of all schemes. The variable x may represent either a monthly mean or a time step value.
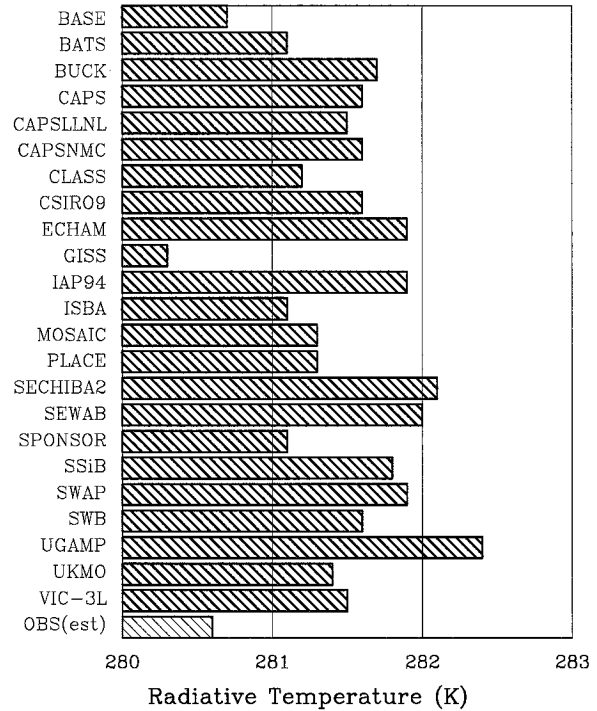

FIG. 2. Annually averaged surface radiative temperature (K).

a. Radiation

The surface net radiation is given by

$$R_n = (1 - \alpha) R_s + \in R_{ld} - \in \sigma T_r^4, \quad (3)$$

where R_s is shortwave radiation, R_{ld} is downward longwave radiation, T_r is surface radiative temperature, α is surface albedo, $\in$ is thermal emissivity, and σ is Stefan–Boltzmann constant. Among the variables and parameters on the right-hand side of (3), only T_r and α vary across schemes; the emissivity was assigned a value of 1. Furthermore, the effective mean, snow-free value of albedo was also prescribed. Given the limited role of snow at this site, it was found that T_r was the main variable explaining variance of R_n across schemes.

Figure 2 shows the annually averaged surface radiative temperature simulated by individual models compared with observations. The observed value was derived from the measurements of upward and downward longwave radiation, R_{lu} and R_{ld}, for each measurement period (30 min)—that is,

$$R_{lu} = \in \sigma T_r^4 + (1 - \in) R_{ld}. \quad (4)$$

The observation point in Fig. 2 was obtained using an emissivity of 1, consistent with the specifications for the model intercomparison; other values of emissivity were used in (4) for the sensitivity analysis to be described later. Most models predict a radiative temperature between 281 and 282 K, which is above the observed value (280.6 K). There is a range of 2 K across models.
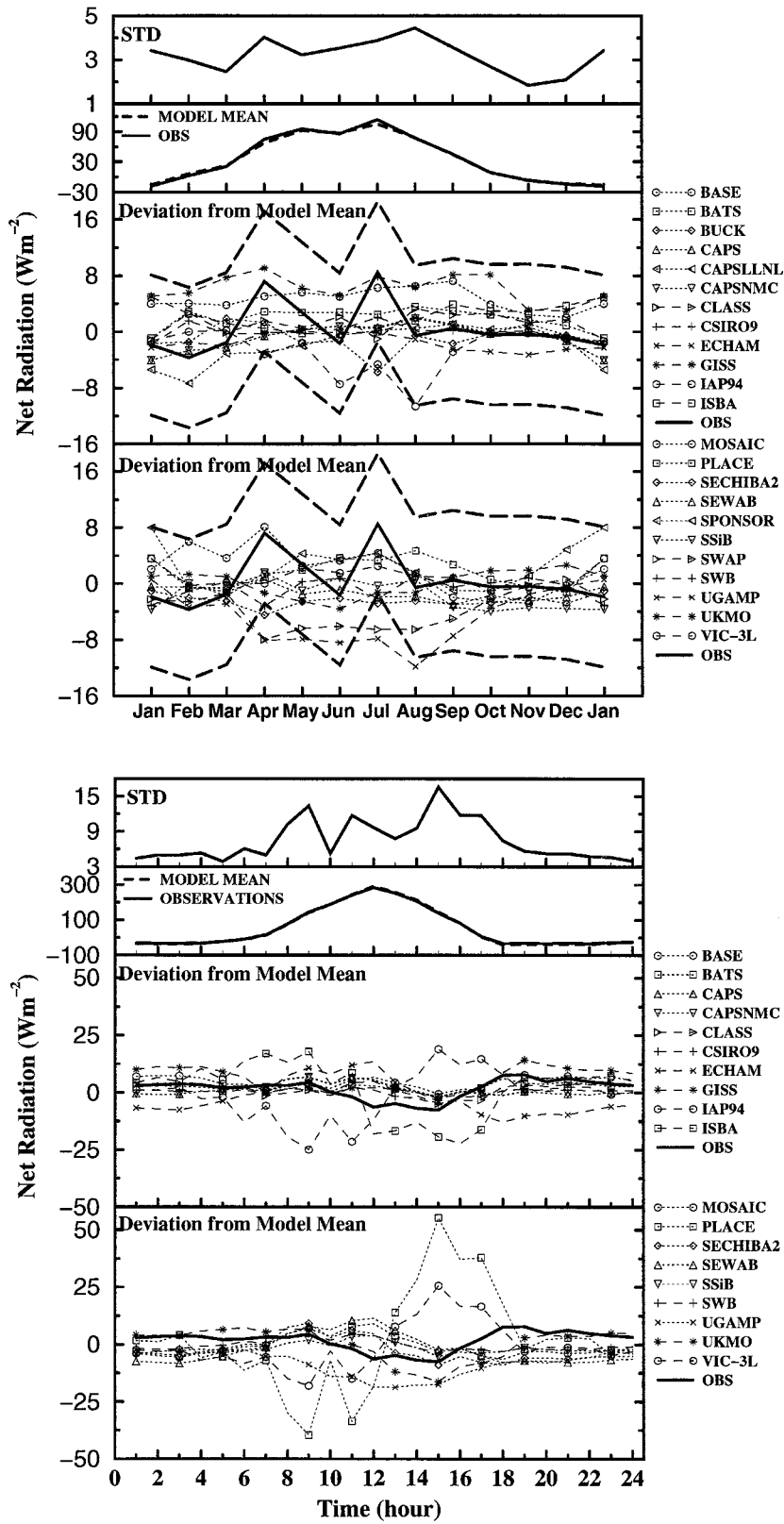
FIG. 3. (a) Seasonal and (b) diurnal (averaged over the 10 days of 10–19 September) variations of surface net radiation (W m^{-2}) for standard deviation across models (panel 1 from the top), model mean and observations (panel 2), and deviations from model mean (panels 3 and 4;

Figure 3 shows the seasonal (Fig. 3a) and diurnal (Fig. 3b) variations of surface net radiation by the three statistics. The STD of monthly net radiation has an average over the year of 3 W m^{-2}. The output from each scheme does not differ from the observation by more than the estimated maximum observation error, except during April, May, July, and August, when some schemes significantly underestimate net radiation. The model mean agrees well with the observations throughout the year, except for April and July. The STD of simulated radiative temperature (Fig. 4a) has an average over the year of 0.6 K. In comparison to the observations, the surface radiative temperature is overestimated by most schemes throughout the year.

At the diurnal scale, the STD of net radiation (Fig. 3b) and that of radiative temperature (Fig. 4b) have averages over the day of 7 W m^{-2} and 0.8 K, respectively. The STD appears to be significantly higher during the daytime from 0800 to 1800 UTC for net radiation and relatively low around 0700 UTC and 1700 UTC for radiative temperature. The latter is explained by the characteristic zero crossings of individual scheme deviations at these times of day, when the sensible heat flux changes sign. This pattern of intermodel deviations could be generated by slight to moderate (5%–25%) differences in effective atmospheric bulk transfer coefficients; such differences are known to exist among schemes, despite the assignment of fixed roughness lengths. Another factor is undoubtedly the variability in effective surface thermal inertia across schemes; this will be discussed later in connection with the diurnal energy fluxes.

Most schemes predict the net radiation with a deviation of less than 10 W m^{-2} from the observations. The diurnal changes in surface radiative temperature simulated by most schemes are roughly in agreement with those observed, but computed values tend to be higher than observed.

IAP94, ISBA, PLACE, and VIC-3L appear to be the outliers from the model population of net radiation in Fig. 3b. The deviations from model mean are easily explained by small phase shifts (on the order of 15 min) of otherwise similar net radiation curves. The evidence suggests these are an unimportant numerical artifact of time accounting differences among some schemes. They do not appear to be correlated with other anomalies noted in the study.

Plots of radiative temperature in Fig. 4a suggest a consistent model or observational bias, averaging 0.87 K across schemes. It is possible that the apparent error in radiative temperature arises partially from the specification of an emissivity of 1 for the surface. If the actual emissivity were constant at 0.95, then the mean radiative temperature inferred from observations by (4) would be 0.5 K higher, or 281.1 K. Sensitivity studies with one model suggest that if an emissivity of 0.95 had been used in the models, computed surface temperature would have been only about 0.2 K higher; the lower sensitivity of the models relative to the measurements is due to the existence of feedbacks in the models, which cause the longwave irradiance to change as surface temperature changes. Extrapolation of these results suggests that the bias would vanish at an emissivity of about 0.86. Since grassland emissivities are likely to be no smaller than 0.95 (Sutherland 1986), it appears that only about one-third of the apparent model bias could be removed if a more realistic emissivity had been used. The discrepancy in radiative temperature could also be due to the fact that none of the models treats the heterogeneity of leaf exposure. The highest protruding elements are cooled most efficiently and are thus cooler than the canopy mean, but because of their topmost position, they contribute a disproportionately large fraction of the upward longwave radiation. They are radiationally dominant over the warmer, more protected, "average" canopy element that most models treat.

b. Latent, sensible, and ground heat fluxes

In Fig. 5, the annual mean sensible and latent heat fluxes for various schemes scatter roughly along a line having a slope of -1 and intercepts of observed R_n ($=H + LE$). Scatter away from the line is associated with differences between modeled and observed R_n, which, in turn, are strongly correlated ($\rho = -0.92$) with differences in annual T_r; the warm bias noted earlier is related to the deficit of net radiation in many models. Scatter along the line in Fig. 5 reflects differences in the surface energy partitioning between latent and sensible heat fluxes. The range in annual mean net radiation is just over 10 W m^{-2}, and the ranges of sensible and latent heat fluxes are about 25–30 W m^{-2}; differences in energy flux partitioning, therefore, account for the larger share of the differences in both heat fluxes.

In fact, a line fitted through the majority of the data points in Fig. 5 (excluding outliers GISS and BUCK, discussed below) slopes less than the 1–1 line. This is because schemes with low LE have a relative shortage of evaporative cooling, leading to warm surfaces and in turn leading rather directly to low R_n, and hence low $H + LE$. Results for BUCK apparently depart from this pattern because that scheme did not include stability adjustments in its bulk transfer relations; this would tend to produce a warmer surface on average. The results for

←

results are split into two panels for easier identification, and the keys for schemes are listed in alphabetical order). The two thick dashed lines in panels 3 and 4 represent the estimated ±10 W m^{-2} observation errors. Four schemes (BUCK, CAPSLLNL, SPONSOR, and SWAP) are excluded from the plots of diurnal variations because they did not resolve diurnal cycle.
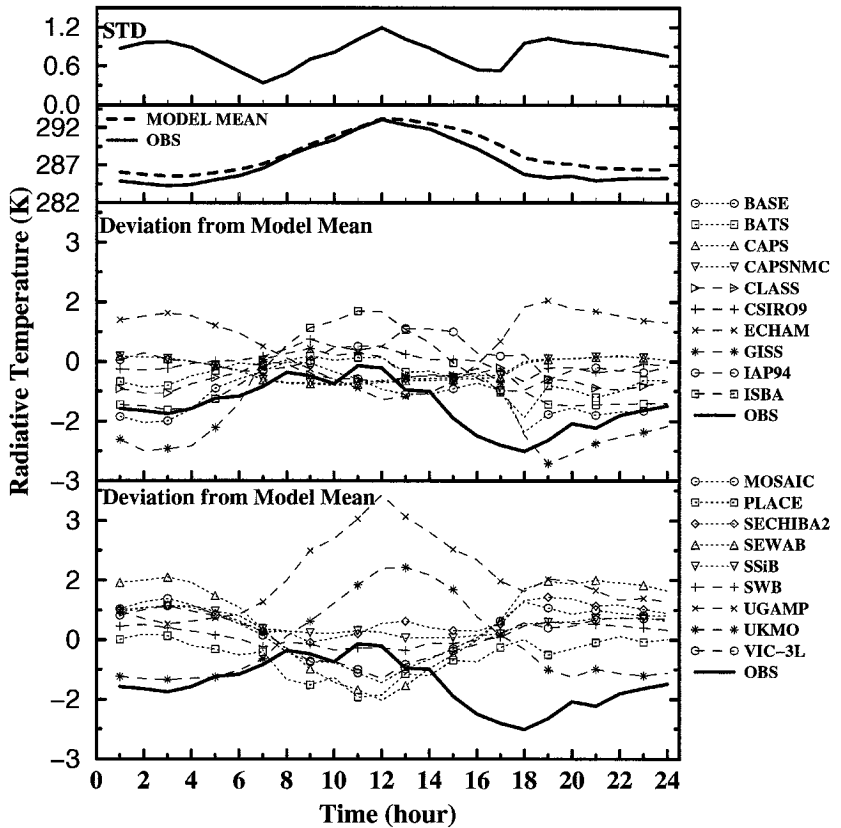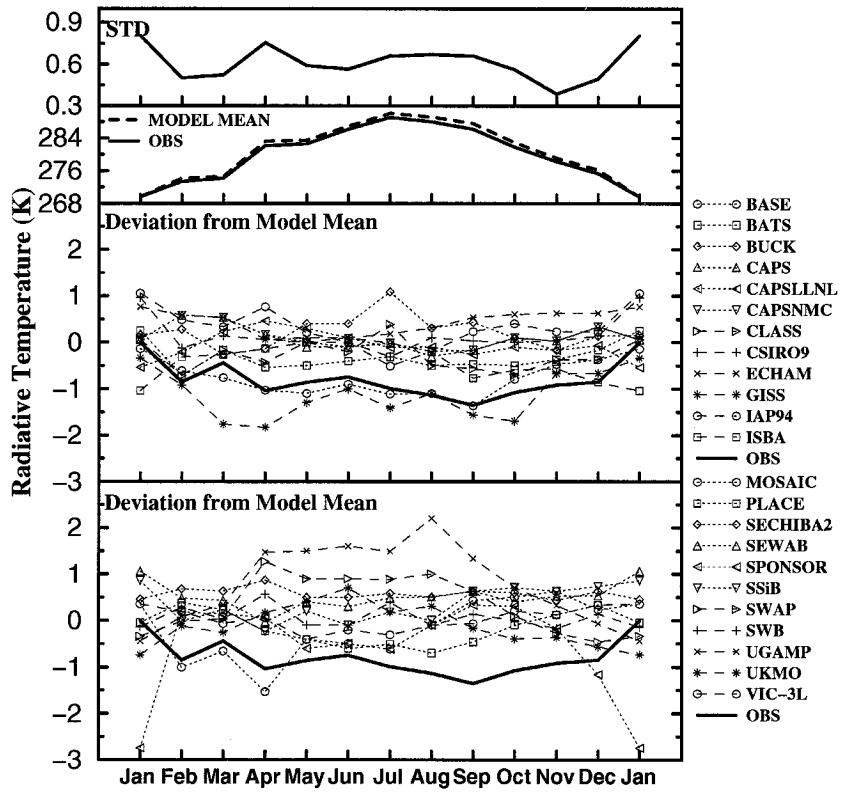
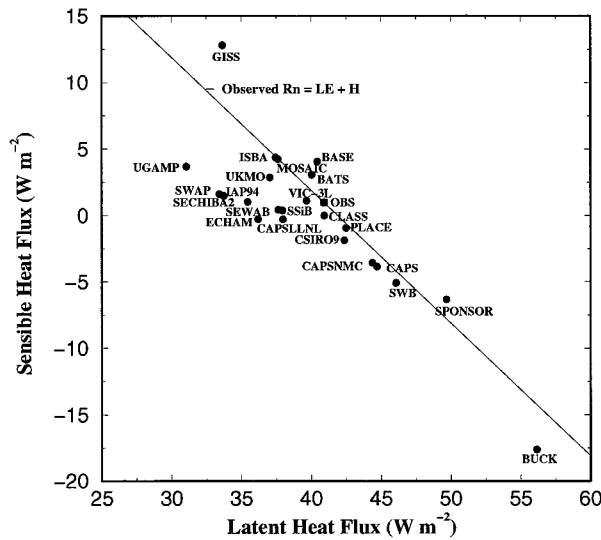FIG. 4. As in Fig. 3 except for surface radiative temperature (K).

FIG. 5. Annually averaged sensible versus latent heat fluxes (W m⁻²). Observed annual mean net radiation (=41 W m⁻²) can be given as the sum of the two coordinates of any single point (latent heat flux + sensible heat flux) on the line.

GISS are possibly affected by numerical difficulties associated with adapting that scheme for the artificial off-line experimental setup required for PILPS; in other (non-Cabauw) PILPS experiments, use of a 30-min time step in GISS has artificially lowered its annual mean temperature (relative to that with a shorter time step) by amounts sufficient to explain the low surface temperature and high net radiation seen here.

We turn now to a brief examination of energy-flux partitioning. The three highest values of latent heat flux (and lowest sensible heat flux) were produced by BUCK, SPONSOR, and SWB. These are the only three schemes in the experiment that effectively ignore the stomatal control of vapor flux under conditions in which water stress is absent. In general, this can be expected to promote latent heat flux and to suppress sensible heat flux when water is freely available. SPONSOR and SWB, unlike BUCK, have stability-related features that tend to suppress downward heat fluxes, and this explains their less extreme position in Fig. 5.

In BUCK especially, it appears that much of the evaporation is supported (energetically) by downward sensible heat flux, suggesting that both fluxes will be very sensitive to the bulk transfer coefficients. A sensitivity test was run with BUCK in which the surface roughness length parameter was changed from the 0.15-m value prescribed for simple schemes to the lower 0.0001-m value prescribed for schemes that use distinct values for momentum and other transfers (see the appendix). Use of the latter value decreased BUCK latent heat flux to 31 W m⁻² and increased sensible heat flux to 2 W m⁻². An identical sensitivity test with one other scheme (SSiB) displayed much smaller sensitivities. On the basis of this and other results, it appears that the strong

sensitivity of BUCK to the roughness parameter is a result of its combined lack of any stomatal resistance and the absence of any adjustment for atmospheric stability.

Aside from GISS, BUCK, SPONSOR, and SWB, discussed above, UGAMP may be identified as a scheme with relatively low latent heat flux, and CAPS and CAPSNMC have relatively high latent heat fluxes; no particular explanation for these fairly small deviations is obvious. It should be noted, though, that the formulations of CAPS and CAPSNMC are very similar in many respects, with differences mainly in runoff processes, and that these schemes were run by a single team for this experiment. The remaining schemes cluster relatively close together near the observations (though with a mean bias that has already been discussed).

The monthly energy balance is

$$R_{nj} - LE_j - H_j - G_j = 0, \tag{5}$$

where j is a month index and G is the sum of surface heat flux into the ground and heat flux into vegetation. Because the canopy heat capacity (see the appendix) is about equal to the heat capacity of a 1-mm layer of soil, the vegetation heat flux can be ignored here. The STD averages 8 W m⁻² for both latent (Fig. 6a) and sensible (Fig. 7a) heat fluxes, or more than double the value for net radiation (Fig. 3a). Relative to the observations, there is a tendency for many schemes to underestimate latent heat flux and overestimate sensible heat flux during summer months, while the reverse holds true during the winter months. Figure 8a shows an average STD of 5 W m⁻² in ground heat flux. The mean across models of predicted monthly ground heat fluxes follows the general course of the observations, but many individual predictions are far outside the range of uncertainty in the observations. In all the three heat-flux variables discussed above, no scheme has estimates that always fall within the range of the observation errors.

Figures 6a and 7a show that the high annual latent heat fluxes (low sensible heat fluxes) seen for BUCK and SWB in Fig. 5 are the result of deviations during the cooler months; during July, in strong contrast, these two schemes have the lowest latent heat fluxes. This result supports the earlier inference that the high evaporation in BUCK and SWB is associated with an absence of surface resistance in periods of low water stress, and it further implies that resultant storage deficits during the warm season inhibit evaporation. For BUCK, the monthly excesses (compared to mean model output) of latent heat flux correlate with wind speed (Fig. 1), giving further support to the earlier conclusion that BUCK fluxes are sensitive to the bulk transfer coefficient. The qualitative similarity between monthly patterns of latent heat flux in BUCK and SWB suggests that SWB results may have a similar explanation of low surface resistance to vapour transfer.

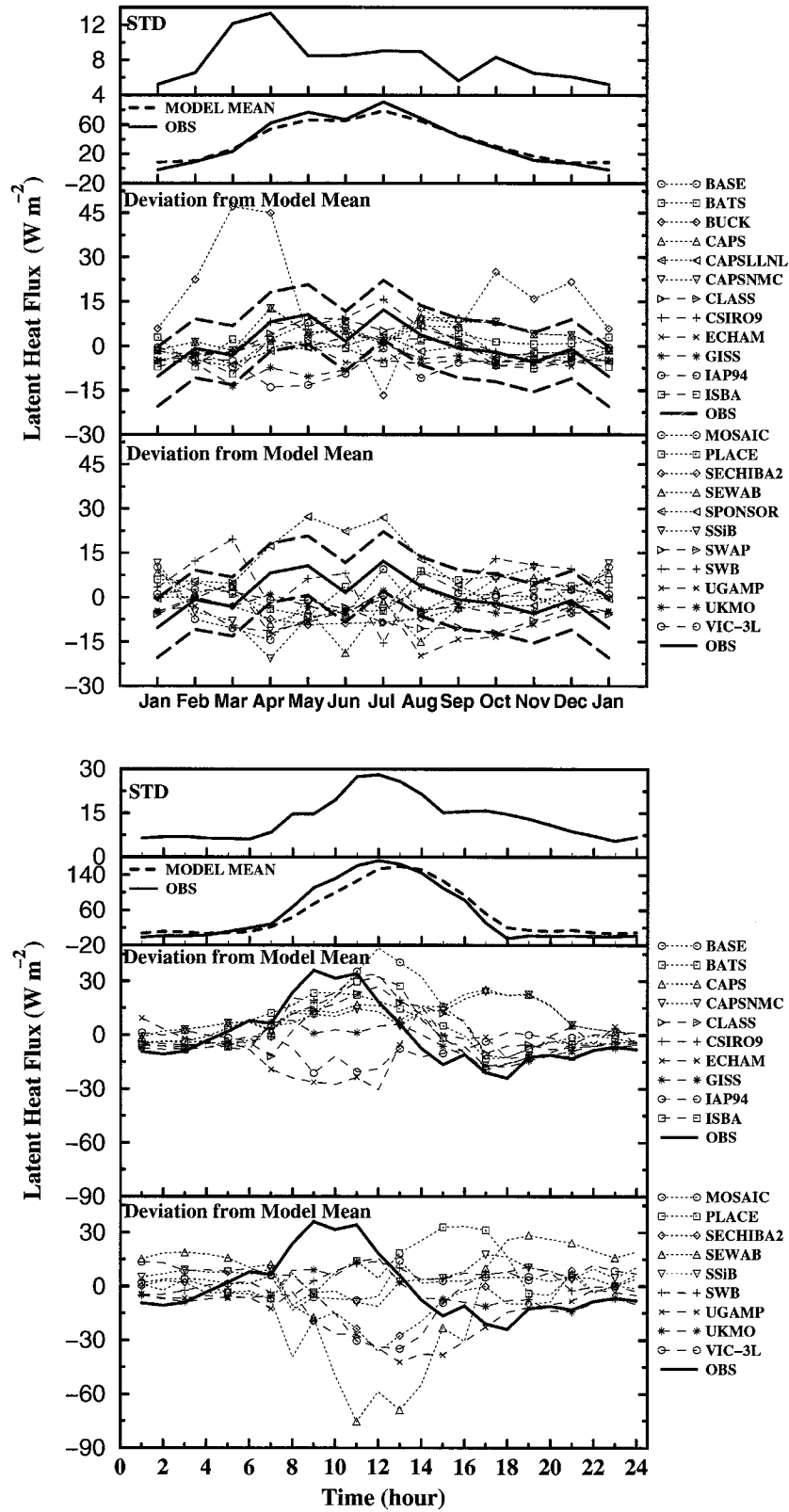In contrast to BUCK, SPONSOR shows anomalously high evaporation (and low sensible heat flux) not in

FIG. 6. As in Fig. 3 except for latent heat flux (W m^{-2}). The two thick dashed lines in panels 3 and 4 represent the estimated ± 10 W m^{-2} observation errors.
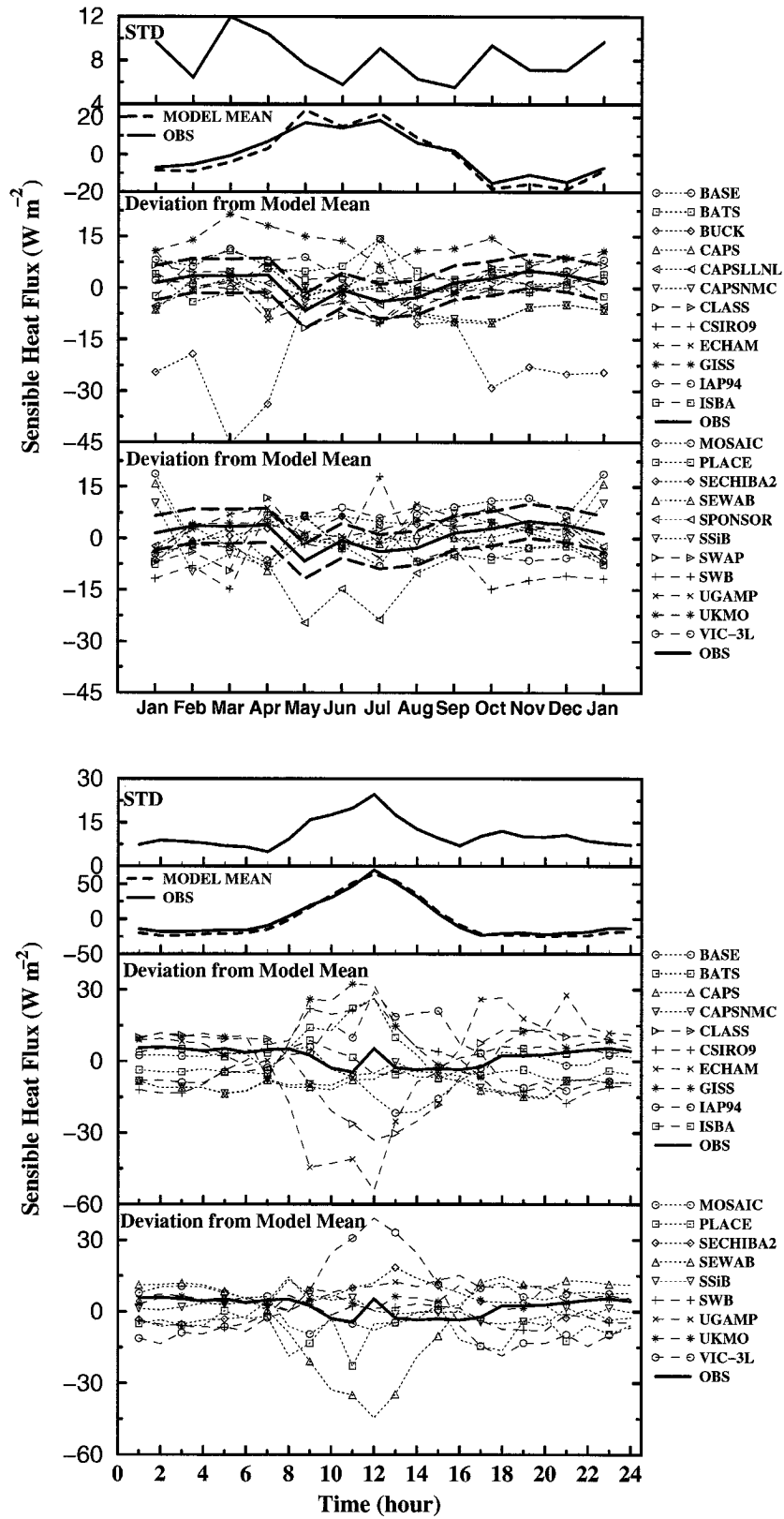
FIG. 7. As in Fig. 3 except for sensible heat flux (W m^{-2}). The two thick dashed lines in panels 3 and 4 represent the estimated ± 5 W m^{-2} observation errors.
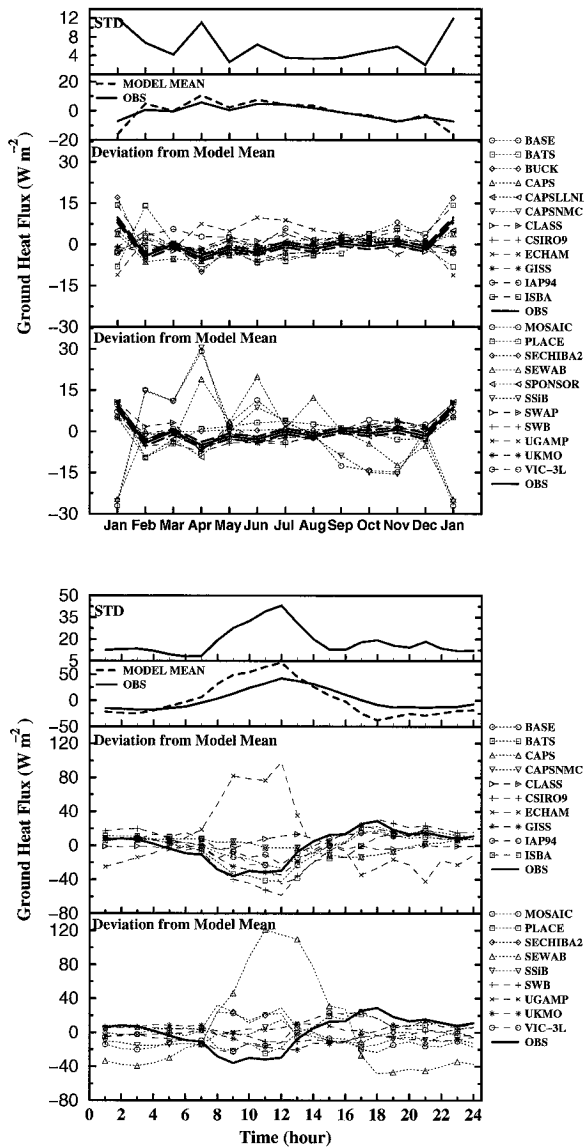
FIG. 8. As in Fig. 3 except for ground heat flux (W m^{-2}). The two thick dashed lines in panels 3 and 4 represent the estimated ±1 W m^{-2} observation errors.

winter, but in late spring and early summer. This is consistent with the fact that SPONSOR neglects stomatal resistance, but also suppresses downward sensible heat fluxes. Hence, SPONSOR tends to have unusually large latent heat fluxes only when there is a strong radiative energy source (and, of course, an available water supply). It is not apparent why the SWB pattern of monthly latent heat flux is not more like that of SPONSOR, given the stability adjustments present in SWB. One possibility is that the two stability formulations used differ significantly in their effects.

Figures 6b, 7b, and 8b illustrate the diurnal cycle of the latent, sensible, and ground heat fluxes. The averages, over the day, of STD are 13 W m^{-2} for latent heat
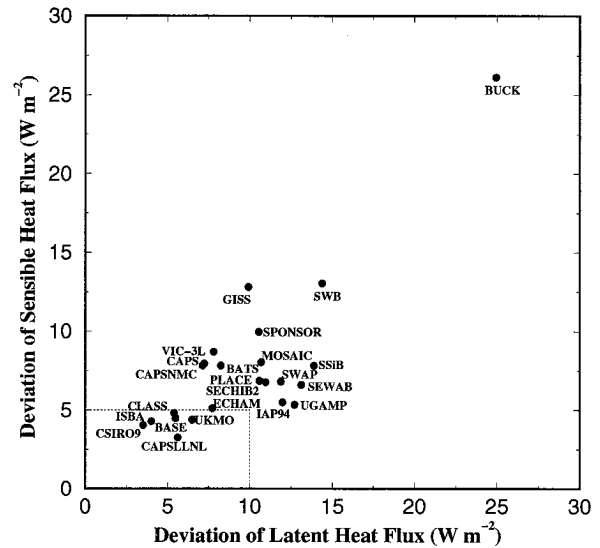

FIG. 9. Averaged rms deviation from monthly observation for sensible versus latent heat fluxes (W m^{-2}).

flux, 11 W m^{-2} for sensible heat flux, and 18 W m^{-2} for ground heat flux. The diurnal variation of STD parallels that of the mean for all three of the heat fluxes, with the highest value around midday (1200 UTC). Compared to the observations, the amplitude of mean modeled ground heat flux is excessive, its peak is early, and the peak of latent heat flux is late. These discrepancies are consistent with those noted by Betts et al. (1993), who attributed them to two deficiencies in the European Centre for Medium-Range Weather Forecasts surface parameterization: insufficient numerical resolution of soil temperature near the surface (amplifying ground heat fluxes and delaying turbulent heat fluxes) and delayed transfer of soil temperature information into the atmospheric boundary layer calculations (causing the early peak in ground heat flux). The first of these problems is a plausible explanation for much of the bias noted here. Variability in numerical representation of soil heat fluxes across schemes is a likely explanation for the cross-scheme variability in diurnal patterns of energy fluxes. We did not attempt to control this aspect of the parameterizations in this experiment, mainly because of the focus on timescales longer than that of the diurnal cycle. This is certainly an area for further attention, but it does not appear that the strength of these deviations in the diurnal cycle was correlated with any characteristics of water or energy fluxes at monthly to annual timescales.

Figure 5 permitted evaluation of the relative accuracy of energy fluxes by schemes, but only on an annual timescale. As a basis for comparing the quality of energy-flux prediction on a monthly timescale, Fig. 9 shows, for each scheme i, the root-mean-square deviation r_i from observation for monthly heat fluxes:
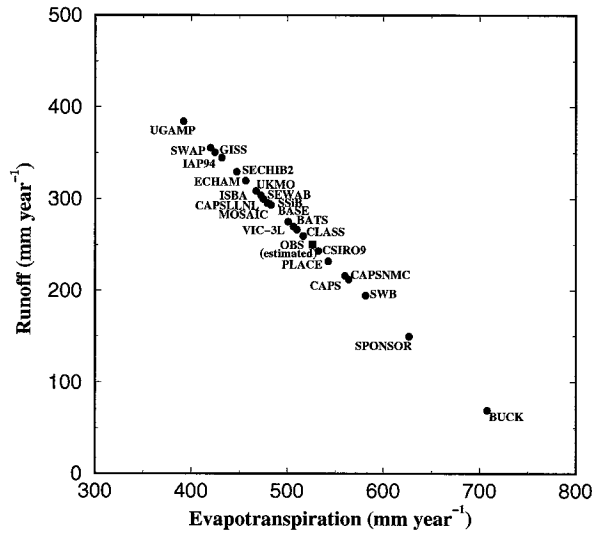
FIG. 10. Annual runoff versus evapotranspiration (mm yr⁻¹).

FIG. 11. Model mean (except precipitation) monthly water balance components (mm month⁻¹).

$$r_i = \sqrt{\frac{1}{12}\sum_{j=1}^{12}(F_{ij} - F_{oj})^2},\qquad(6)$$

where j is a month index, F is latent or sensible heat flux, and subscript o signifies observations. The schemes having predictions that lie closest to the observations in Fig. 5 are not consistently those with the smallest errors in Fig. 9. Six schemes (BASE, CLASS, CSIRO9, CAPSLLNL, ISBA, and UKMO) have rms deviations from observations that are smaller than the estimated upper bounds on observational errors. Here and elsewhere, it must be kept in mind that it is unknown to what extent these results depend on systematic or scheme-specific errors in parameter assignments. In many cases, modelers were not provided with the Cabauw site measurements needed to assign proper values to certain parameters. As a result, these parameters may have been assigned inappropriate values.

There is a range across schemes of about 10 W m⁻² in simulated annual net radiation. The range of simulated latent heat flux and sensible heat flux, between which the net radiation is partitioned, however, is more than two times larger. To appreciate fully the significance of this range, it is informative to go beyond the surface energy balance and explore the surface water balance.

c. Surface water budget

Figure 10 shows the annual partitioning of precipitation between runoff and evapotranspiration [see (2)] for all schemes. The points scatter along a line having a slope of -1 and intercepts equal to the annual precipitation. As shown in Figs. 5 and 10, there is a range across schemes of 25–30 W m⁻² in the annual mean latent and sensible heat fluxes, and a range of 315 mm in both evapotranspiration and runoff. These values are

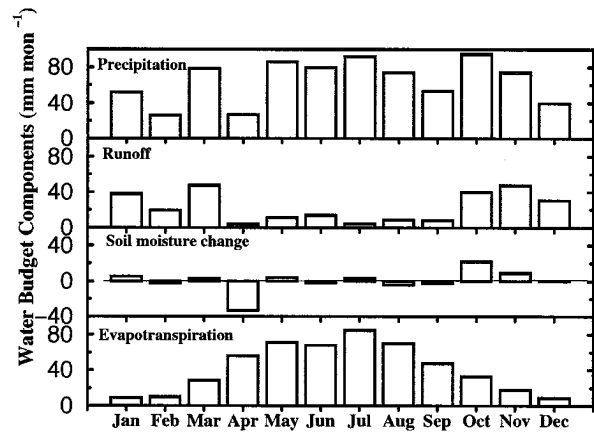related through the latent heat of vaporization of water (about 2.45×10^6 J kg⁻¹). Similarly, observed annual latent heat flux is equivalent to annual evapotranspiration of 526 mm. This implies a residual annual runoff of 250 mm, given the observed precipitation of 776 mm and ignoring net changes in water storage during 1987. These water fluxes are shown in Fig. 10; the observation lies within the scatter of the scheme predictions.

The monthly water balance is

$$\Delta M_j = P_j - E_j - Y_j,\qquad(7)$$

where j is a month index and ΔM_j is the change in total water (in the root zone, on canopy, and in snowpack) storage from the start to the end of month j. To a close approximation, this is the same as the change in root-zone storage, except during months of significant change in snowpack.

The relative magnitudes of components of the surface water balance vary significantly through the seasonal cycle. Figure 11 shows the monthly water balance averaged across all schemes; the overall seasonal patterns in all schemes are similar in evapotranspiration, as can be seen by comparing standard deviations to mean in Fig. 6a, and to a lesser extent, in runoff, as can be seen in Fig. 12. Furthermore, the storage change term is relatively small in all schemes through most times of the year (except for April and October), as a comparison of Figs. 11 and 13 shows. According to Fig. 11, then, most schemes have an excess of precipitation over (apparently non-water-stressed) evapotranspiration from October through March, leading to a runoff production of 20–45 mm month⁻¹, with a standard deviation averaging 12 mm month⁻¹ during the same period. During this season, the monthly march of runoff closely follows that of precipitation. The reduction in runoff to about 10 mm month⁻¹ or less for the months of April through September is associated with the heightened values of non-water-stressed evapotranspiration during this period, when almost all precipitation is consumed by evapo-
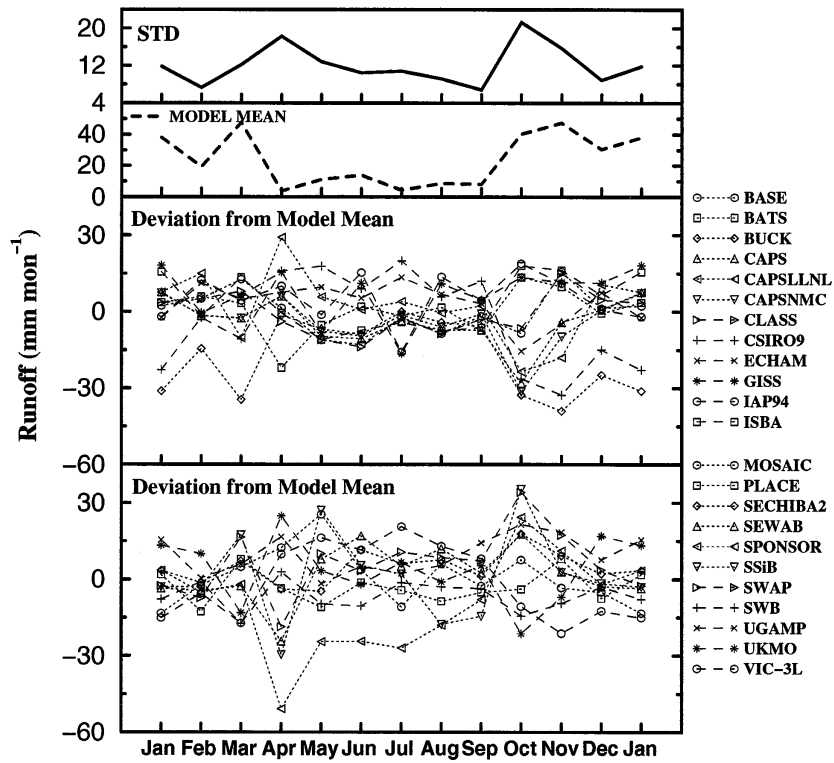
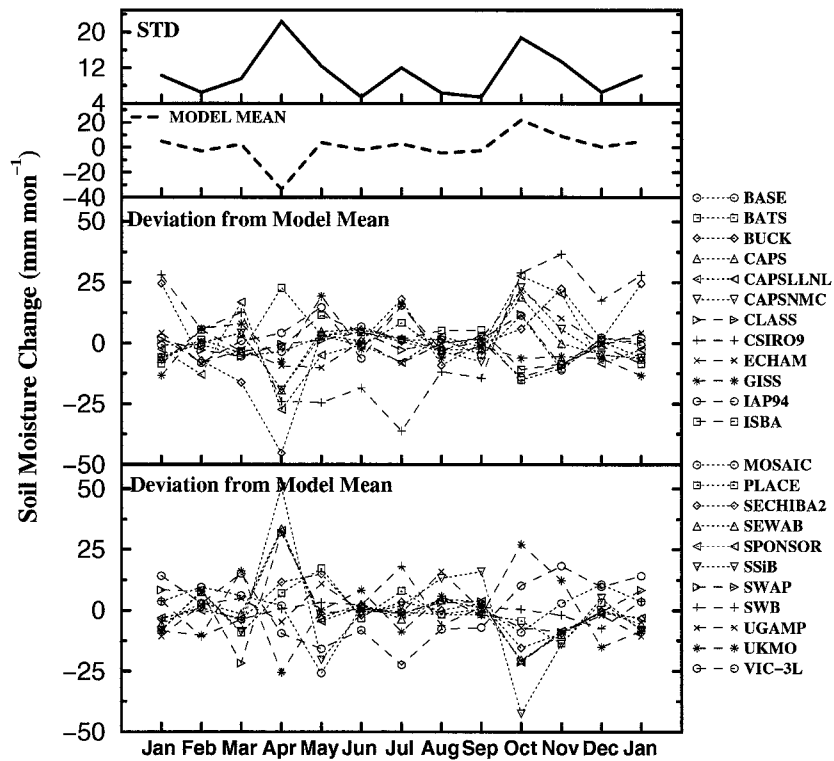FIG. 12. As in Fig. 3a except for modeled runoff (mm month⁻¹).

FIG. 13. As in Fig. 3a except for modeled root-zone (1 m) soil moisture change (mm month⁻¹).

transpiration. The periods of high and low runoff are separated by months of significant storage increase in October and decrease in April. These seasonal patterns of fluxes and storage changes are consistent with a simple conceptual model (e.g., Milly 1994a,b) having soil-moisture storage near some maximum sustainable value (i.e., "field capacity") in winter, storage depletion in spring, storage below field capacity in summer, and storage replenishment in fall.

Beyond the general similarities noted above, the schemes do differ quantitatively in their monthly partitioning of precipitation into storage change (average STD of 11 mm month^{-1}), runoff (12 mm month^{-1}), and evapotranspiration or latent heat flux (9 mm month^{-1}). (For comparison with energy fluxes, 1 mm month^{-1} is approximately equivalent to 1 W m^{-2}.) The largest monthly STDs (about 20 mm month^{-1}) are associated with runoff and storage change and occur during the months of April and October. These are months when, on average across schemes, the runoff season is ending or starting; some variability across schemes in the timing of these seasons could easily explain these maxima. Close examination of Figs. 12 and 13 reveals a significant negative cross correlation between deviations of runoff and storage change during April and October. This implies that the variability during these transition months results not so much from variability of non-water-stressed evapotranspiration, but from differences in model parameterizations of soil water, runoff, and their interaction.

Another notable feature seen in Figs. 12 and 13 is the stronger seasonal cycle of storage and associated weaker seasonal cycle of runoff for CSIRO9 and VIC-3L, which may be indicative of a stronger propensity of those schemes to produce runoff even in the presence of a water-storage deficit. This suggestion will be revisited later in the discussion of modes of runoff and storage of soil water. The winter runoff deficit in BUCK and the summer runoff deficit in SPONSOR seen in Fig. 12 are directly connected to the contemporaneous high values of latent heat flux already discussed in connection with Fig. 6a.

As discussed earlier, winter (November–March) evapotranspiration is probably not limited by water supply in most schemes. This implies that the variability of evapotranspiration during this season is controlled by variability of energy supply, non-water-stressed surface resistance to vapor transport, and aerodynamic transport parameterizations across schemes. The resulting variability of water surplus (precipitation minus evapotranspiration) must be amplified by differences in soil-moisture and runoff parameterizations to produce the somewhat higher variabilities of runoff and storage changes.

The importance of soil-water stress during summer (May–September) is not clear; it may or may not be a factor in any given scheme. The near equality of precipitation and evapotranspiration is suggestive of possible water limitation, but the average root-zone soil-water decrease from winter to summer is only about 40 mm. The absence of a significant summer peak in the latent-heat-flux variability supports the hypothesis that even summer evapotranspiration variability is largely controlled by factors other than water availability. It would follow that variability of annual mean runoff across schemes is determined directly by the variability in the difference between annual means of precipitation and non-water-stressed evapotranspiration; this is simply the variability in evapotranspiration, because precipitation is constant across schemes. In addition to this, differences in soil-moisture and runoff parameterizations determine the timing of runoff through the year, explaining part of the variance of monthly runoff and storage change.

It is not surprising that the Cabauw site might experience little water stress throughout the year, given the presence of a shallow water table. However, based on a review of experimental procedures, it appears that this water source was ignored in over half of the schemes; most schemes retained their assumption of free gravity drainage of the soil column. This assumption is standard in schemes designed for use with atmospheric models. The apparent rarity of water stress in most models appears to have arisen simply from the near adequacy of the water supply (precipitation and stored soil water) to meet evaporative demands.

No overland flow has been observed at Cabauw. Furthermore, the terrain is flat, so lateral flow in the root zone ("interflow") is not expected to be an important term in the water balance. Rather, essentially all excess water drains to the water table and is thereafter transported laterally through the saturated zone to the drainage ditches. Figure 14 shows how the annual runoff computed by each scheme was partitioned into vertical flux across the bottom of the root zone ("drainage," which could be negative if the water table is a net source of water to the root zone) and the sum of interflow and overland flow; interflow and overland flow are not separated in the figure because they had been lumped together when model results were reported. (Participants running BUCK and SECHIBA2 specified that total runoff should not be differentiated by type; for Fig. 14, we assigned all runoff to drainage in these cases because of the use of the field capacity concept in these schemes.)

As shown in Fig. 14, many schemes include a significant component of runoff by overland flow or interflow. The absence of drainage in CLASS can be understood in terms of how it was set up for this particular experiment; the water-table boundary condition was treated as a no-flow condition, preventing drainage of the soil and requiring runoff by other routes. Three schemes (SPONSOR, SEWAB, and MOSAIC) produced much overland flow and drew water from the water table in the annual mean to achieve a balance. The large amount of overland flow in MOSAIC was
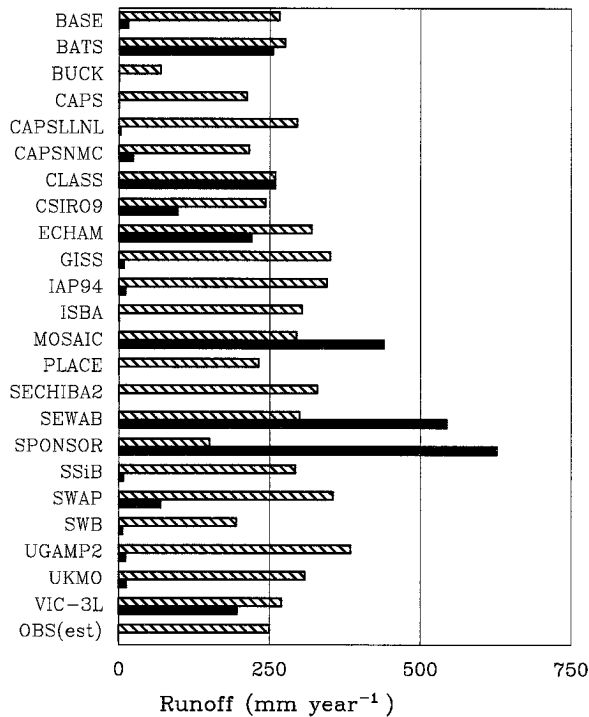
FIG. 14. Annual values of total runoff (diagonally hatched bar) and the sum of overland flow and interflow (solid bar). (Drainage is equal to total runoff minus the sum of overland flow and interflow; it is negative in MOSAIC, SEWAB, and SPONSOR.) Values are in mm yr^{-1}.

FIG. 15. Annually averaged root-zone (1 m) soil moisture (mm).

caused by a parameterization designed to represent partial-area saturation at the subgrid scale of GCMs; it may not have been appropriate for use at the relatively small and homogeneous Cabauw site. In contrast, high overland flow from SPONSOR and SEWAB appears to have resulted from an excessive influence of the water table on root-zone water content, which was near saturation at least most of the year in those schemes. High water content promotes surface runoff by minimizing the pore volume available to receive infiltration. In the case of SPONSOR, the cause of this "waterlogging" was a nonphysical parameterization of soil water flow, which has since been replaced. For the remaining four schemes (BATS, CSIRO9, ECHAM, and VIC-3L) having a significant fraction of runoff by modes other than drainage, the most likely explanation appears to be a propensity for surface runoff production under nonsaturated root-zone conditions. For CSIRO9 and VIC-3L, this inference is consistent with their anomalous monthly patterns of runoff and water storage, noted already in connection with Figs. 12 and 13.

d. Soil moisture

During the planning of the PILPS phase 2a experiment, it was anticipated that the high water table at the Cabauw site would tend to "anchor" modeled values
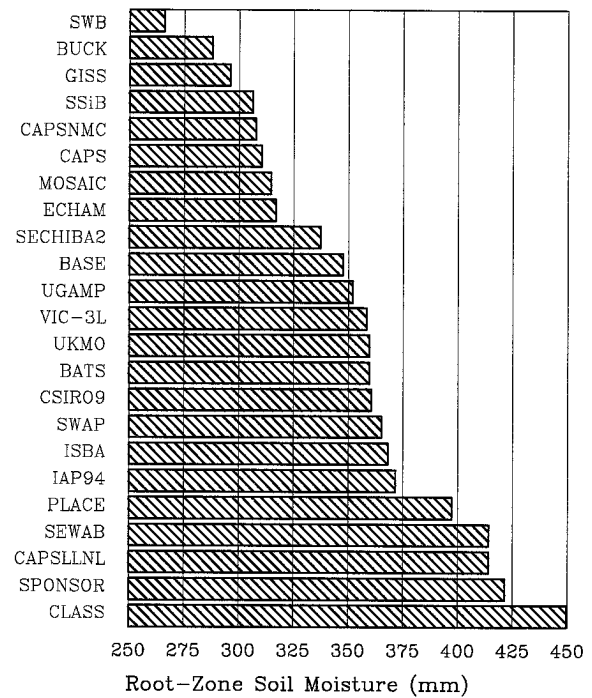
of soil moisture and, therefore, to minimize differences in soil moisture among schemes. However, as shown in Fig. 15, there is a range of 184 mm across schemes in the simulated root-zone soil moisture; this is equivalent to 24% of annual precipitation or 40% of total pore volume. Apparently, the water-table boundary condition did little to reduce the spread; as pointed out above, it turns out that at least half of the models were run under a standard assumption of free soil drainage by gravity, which is equivalent to a very deep water table having no influence on surface conditions.

Analyses were conducted to determine how much of the variances of annual soil moisture or energy- and water-flux partitioning could be explained by the differing boundary conditions. No significant amount of cross-scheme variance was explained in any of these analyses. Nor was soil moisture a significant predictor of flux partitioning. (The latter result can be explained partially by the fact that relations between moisture content and fluxes, though qualitatively similar, often differ quantitatively across models.) However, in individual cases, it is possible to explain the extreme values of root-zone soil moisture with reference either to features of the schemes or to how they were set up for the experiment. On the basis of a survey of participants, it appears that PLACE is the only scheme that was given a physical boundary condition consistent with a water table at 1-m depth, and the resulting water content is consistent with expectations, as the discussion below will show. The vertical no-flow condition used in CLASS at the bottom of the modeled soil depth, noted

earlier in the explanation of runoff, maintained the root zone at a moisture content near saturation. The strong water-table influence in SEWAB and SPONSOR had a similar effect. The high evaporation in BUCK and SWB, in the absence of water-table support, caused those schemes to have the lowest water contents of all schemes; a similar argument may also explain the moderately low soil moisture in CAPS and CAPSNMC. Relatively low water content in MOSAIC is associated with the subgrid production of surface runoff, as already discussed.

Unfortunately, no measurements of soil moisture were available for evaluating the various model outputs in this project. But lacking such data, one can at least make some comparisons with theoretical limiting cases that would be consistent with the specified soil properties. Assuming that runoff, as observed (Beljaars and Bosveld 1997), is by soil drainage, the modeled winter runoff rate of about 1 mm day^{-1} can be equated to an unsaturated hydraulic conductivity to estimate an expected winter water content in those models assuming free drainage. This implies a root-zone water content of about 370 mm. If the summer value is 40 mm lower (Fig. 11), then the annual average would be about 350 mm. For a water table at 1-m depth, on the other hand, a hydrostatic soil-moisture profile can be shown to contain 390 mm of water in the root zone; for a shallow water table, the mean storage will not differ much from the equilibrium storage (Salvucci and Entekhabi 1994). The difference in water storage associated with different boundary conditions (40 mm) is much smaller than the range of values found in this project (184 mm). This may explain why no significant relation was found between annual soil moisture and the type of boundary condition applied.

On the basis of these theoretical analyses, and allowing for some errors in them, it is expected that annual mean values of root-zone soil moisture will be between 330 and 410 mm. It is interesting that the center of this range agrees quite well with the central cluster of schemes in Fig. 15. As already noted, many of the higher and lower values can be explained in terms of experimental setups or anomalous evaporation rates. In some cases, it appears that other significant departures from the expected range may be explained by use of soil properties different from those specified for the experiment.

5. Concluding remarks

The PILPS phase 2a experiment, described in this paper, was conducted using observed data (downward shortwave and longwave radiation, precipitation, and near-surface air humidity, temperature, and wind speed) for the year 1987 from Cabauw as inputs to a variety of land-surface schemes. Schemes were evaluated by comparing their outputs with long-term measurements of surface sensible heat fluxes into the atmosphere and

the ground, and of upward longwave radiation and total net radiative fluxes, and with latent heat fluxes derived from a surface energy balance. The observation that no overland flow occurs at the site also served as a data point to check model performance. Tuning of schemes by use of the observed flux data was not permitted.

Twenty-three land-surface schemes have participated in the experiment. Analyses of the experimental results were focused on the energy budget, the water budget, and their linkage. Although all schemes used identical atmospheric forcing data and the land-surface parameters were specified with great care, the differences in experimental results among the land-surface schemes and observations were found to be significant. The magnitudes of differences for some recognized key variables are qualified and discussed below.

1) On an annual mean basis, there is a range across schemes of about 10 W m^{-2} in simulated net radiation, which is associated with the range of 2 K in the surface radiative temperature. Annual means of sensible and latent heat fluxes, into which net radiation is partitioned, have ranges across schemes of 30 W m^{-2} and 25 W m^{-2}, respectively. Annual totals of evapotranspiration and runoff, into which the precipitation is partitioned, both have ranges of 315 mm. These ranges of energy- and water-flux partitioning are, of course, related directly through the latent heat of vaporization of water. Three schemes do not include any explicit stomatal resistance under non-water-stressed conditions; these produce the three highest latent heat flux (evaporation) values. When these schemes are excluded, the ranges of annual heat and water fluxes are approximately halved.

2) The STD of simulated monthly net radiation has an average over the year of 3 W m^{-2}. This difference is mainly attributed to the simulated surface radiative temperatures, which have an average STD of 0.6 K. The predicted net radiation from each scheme does not differ from the observation by more than the estimated observation error ($\pm$10 W m^{-2}) through most of the year. Models appear to systematically overestimate the observed radiative surface temperature. This discrepancy may be associated with erroneous assumptions about surface emissivity in the experiment and with the models' neglect of canopy thermal heterogeneity.

3) The STDs of both monthly latent and sensible heat fluxes average 8 W m^{-2} over the course of the year. The most significant deviations from monthly observations are associated with the three schemes that neglect non-water-stressed stomatal resistance. Relative to the observations, there is a tendency for many schemes to underestimate latent heat flux and overestimate sensible heat flux during summer months, while the reverse holds true during the winter months. The monthly ground heat flux at the surface has an average STD of 5 W m^{-2}. The mean

across models of predicted ground heat fluxes follows the general course of the observations, but, in many cases, individual predictions are far outside the estimated range of uncertainty in the observations (± 1 W m^{-2}).

For 6 schemes, root-mean-square deviations of predictions from monthly observations are less than 5 W m^{-2} for sensible heat flux and 10 W m^{-2} for latent heat flux, which are the estimated upper bounds on observation errors. However, the extent to which these results depend on systematic or scheme-specific errors in parameter assignments is unknown.

4) To reconstruct a typical diurnal cycle, time step outputs have been averaged across 10 days (10–19 September). Values of STD, defined with respect to 10-day mean time step values, average 7 W m^{-2} for net radiation, 0.8 K for radiative temperature, 13 W m^{-2} for latent heat flux, 11 W m^{-2} for sensible heat flux, and 18 W m^{-2} for ground heat flux, with the highest variances around midday (1200 UTC) in all these variables. Most schemes predict the net radiation with a deviation of less than 10 W m^{-2} from the observations. The diurnal changes in surface radiative temperature simulated by most schemes are roughly in agreement with those observed, but computed values tend to be higher than observed, as discussed already in connection with the monthly values. During the daytime, there is a distinct phase shift of modeled latent and ground heat fluxes relative to the observations. In the models there is a tendency for latent heat flux to peak late and for ground heat flux to peak early. In contrast, the phase of the mean model output appears correct for sensible heat flux. Deviations in diurnal patterns of temperature and energy fluxes are most likely associated with different numerical treatments of soil thermal inertia. These deviations on the diurnal timescale do not appear to be correlated with (nor, in particular, causative of) deviations on longer (e.g., monthly) timescales.

5) Schemes differ in their partitioning of precipitation into evapotranspiration, storage change, and runoff. Monthly values of STD average 9 mm month^{-1} (8 W m^{-2}) for evapotranspiration (latent heat flux), 11 mm month^{-1} for storage change, and 12 mm month^{-1} for runoff. The variability across schemes of runoff and storage change is largest (about 20 mm month^{-1}) during April and October, which are months of transition between high and low (or negligible) runoff. This is largely attributable to the differences in the model parameterizations of soil water, runoff, and their interaction. In winter, when evapotranspiration is not limited by water availability, variance of water surplus (precipitation minus evapotranspiration) is amplified by differences in soil-moisture and runoff parameterizations.

6) The partitioning of annual runoff into its physical components was examined. Observational evidence and site topography suggest that overland flow and interflow are negligible, leaving vertical drainage to the water table and subsequent groundwater discharge as the main mode of runoff at the site. However, the schemes differ widely in their modes of runoff. In some cases, the production of overland flow can be understood in terms of the details of how a scheme was set up (nonoptimally) for the experiment. In several other cases, however, it appears that schemes have an inherent propensity to produce overland flow that is inconsistent with the observations. The apparent insensitivity of total runoff to its physical partitioning may be explained by the rarity of water stress at the site; in the long run, runoff is the difference between precipitation and non-water-stressed evapotranspiration.

7) On an annual basis the simulated root-zone soil moisture has a range across schemes of 184 mm (40% of total pore volume). No field data were available for evaluating modeled soil moisture. However, this range of model values did appear to be wider than what could be accounted for theoretically. No consistent relation was found between the scatter in the predicted root-zone soil moisture and that in any of the energy- and water-flux variables analyzed in this study. This is not surprising, in view of the large variety of relations between fluxes and water content that is found across models. It implies that the demonstration of the ability of a scheme to reproduce observed water content changes does not necessarily establish its ability to reproduce water and energy fluxes. In nearly all cases, however, it was possible to explain the most extreme values of soil moisture in terms of the particulars of the experimental setup or excessive evapotranspiration.

The discrepancy between simulations and observations could be due to a number of reasons: for example, neglected physical processes in the models, uncertainty about important parameter values required by some schemes, lack of detailed descriptions of the specific conditions in Cabauw, lack of atmospheric forcing data before the year that would allow appropriate spinup, or the assumption that PILPS's offline simulations are comparable with point observations.

In this study, the availability of a full year of observed energy flux data was a major advantage. The absence of appropriate runoff and soil moisture data for the study year, on the other hand, was a serious shortcoming, especially in view of the spread of results for runoff and water storage. Furthermore, it would have been useful to demonstrate from the experimental point of view the accuracy with which the surface water budget is closed.

The focus of this paper has been on a community-wide intercomparison among models. A detailed analysis of each model is beyond the scope of this study. However, the information given in this paper should

serve as a reference for individual modeling groups to explore their model behaviors in this experiment.

APPENDIX

Site Characteristics and Parameter Setup

In PILPS phase 2a experiment, a set of parameters was derived from a variety of sources in an attempt to characterize the Cabauw site fully. Where possible, these parameters were obtained from site-specific information. When a parameter was not available from site-specific observations, typical values were assigned on the basis of the standard set of parameter in BATS (Dickinson et al. 1993) or the Simple Biosphere Model (Sellers et al. 1986). The parameter values were classified into four groups, as given below.

a. Soil properties

Soil is silty clay with negligible surface slope. Soil physical characteristics were assumed spatially homogeneous and temporally invariant. It was assumed that soil-water flow can be treated using the single-continuum approach common in theoretical soil physics. Soil hydraulic and thermal properties for Cabauw, described by Beljaars and Bosveld (1997), were not known to PILPS at the time the numerical experiments were designed and run. The hydraulic properties were assigned on the basis of a misinterpretation of results of Cosby et al. (1984), which caused the assigned air-entry suction and saturated hydraulic conductivities to be scaled by factors of 0.14 and 2.6, respectively, relative to what they would have been if they had been assigned values central to the populations of parameters analyzed by Cosby et al. (1984) for silty clay. However, the reported spread of those populations was so large that the parameters used here are not atypical of a silty clay. Soil thermal properties are assumed to be those specified by BATS for its silty clay soil type. Bare-soil roughness length was assigned a value typical for soils. The parameters are listed in Table A1.

With the soil physical parameters above and the matric head at the wilting point of the vegetation (see the

TABLE A1. Parameters describing soil properties.

Soil porosity	0.468
Saturated hydraulic conductivity (m s^{-1})	3.4341×10^{-6}
Air-entry suction (mm)	45
"B" of Clapp and Hornberger (1978)	10.39
Ratio of thermal conductivity to that of loam	0.75

following section), the water content of the root zone at wilting point is 214 mm.

In models treating the root zone as a single water store, the effective water capacity was set to 150 mm, following Manabe (1969). An independent estimate was obtained by determining, using an approximate analytic solution of the Richards equation, the amount of evapotranspiration that could occur, following soil saturation, before gravity-induced drainage caused the water content to drop to the wilting point, given typical non-water-stressed rates of evapotranspiration. (In the context of a simple storage model, this amount of evaporation would be identical to the effective water capacity.) The estimates derived by this approach did not differ by more than 10–20 mm from the value of 150 mm. Adding this standard value to the "unavailable" water content at wilting yields an estimate (364 mm) of root-zone soil moisture at the free-gravity-drainage field capacity of the soil. This is consistent with the estimated winter water content under free drainage (370 mm) given in the text.

For models without explicit water-stressed stomatal control of transpiration, the critical water content, above which evapotranspiration equals the non-water-stressed rate, was taken to be 75% of the effective capacity.

b. Vegetation properties

Vegetation is short grass. The root distribution placed 70% of the total roots in the top 0.1 m and all remaining roots in the next 0.9 m. The parameters are listed in Table A2.

c. Radiative transfer characteristics

Snow-free albedo of site was specified as being 0.25 (Duynkerke 1992) in those models that use albedo as a parameter. Parameters of models with more detailed treatment were set in an attempt to match an overall albedo of 0.25. Albedo of fresh snow was taken as being 0.75. Other parameters are listed in Table A3.

d. Aerodynamic transfer characteristics

Aerodynamic transfer characteristics were based mainly on the vegetation structural properties. The momentum roughness length was set to 0.15 m (Beljaars and Bosveld 1997) and the zero-plane displacement height to zero. Roughness lengths for heat and moisture

TABLE A2. Parameters describing vegetation properties.

Leaf area index

Jan	Feb	Mar	Apr	May	Jun	Jul	Aug	Sep	Oct	Nov	Dec
0.8	1.0	1.1	1.3	1.6	1.8	1.8	1.6	1.5	1.1	1.0	0.9

Fractional vegetation cover

Jan	Feb	Mar	Apr	May	Jun	Jul	Aug	Sep	Oct	Nov	Dec
0.92	0.93	0.94	0.95	0.97	0.98	0.99	0.98	0.97	0.96	0.95	0.93

Green leaf fraction

Jan	Feb	Mar	Apr	May	Jun	Jul	Aug	Sep	Oct	Nov	Dec
0.85	0.88	0.89	0.91	0.92	0.93	0.83	0.86	0.67	0.81	0.79	0.77

Maximum height of vegetation (m)	0.2
Height of maximum canopy density (m)	0.15
Stem area index	4
Minimum stomatal resistance (s m^{-1})	40
Maximum stomatal resistance (s m^{-1})	20 000
Interception capacity (mm)	0.1 × LAI
Canopy heat capacity (J m^{-2} K^{-1})	2000
Soil-water matric head at wilting (m)	150

TABLE A3. Parameters describing radiative transfer characteristics.

Visible (shortwave) albedo of canopy	0.15
Near-infrared (NIR) albedo of canopy	0.35
"Visible" albedo of fresh snow (>0.7 μm)	0.65
NIR albedo of fresh snow (<0.7 μm)	0.85
Thermal emissivity of all surface components	1

TABLE A4. Parameters describing aerodynamic transfer characteristics.

Von Karman constant	0.378
Momentum roughness length of bare soil (m)	0.001
Momentum roughness length of snow on ground (m)	0.0024

were set equal to that for momentum in some models, but to 0.0001 m (Beljaars and Holtslag 1991) in those models that allow different values. Other parameters are listed in Table A4.

REFERENCES

Abramopoulos, F., C. Rosenzweig, and B. Choudhury, 1988: Improved ground hydrology calculations for global climate models (GCMs): Soil water movement and evapotranspiration. *J. Climate,* **1,** 921–941.

Beljaars, A. C. M., 1982: The derivation of fluxes from profiles in perturbed areas. *Bound.-Layer Meteor.,* **24,** 35–55.

——, and A. A. M. Holtslag, 1991: Flux parameterization over land surfaces for atmospheric models. *J. Appl. Meteor.,* **30,** 327–341.

——, and P. Viterbo, 1994: The sensitivity of winter evaporation to the formulation of aerodynamic resistance in the ECMWF model. *Bound.-Layer Meteor.,* **71,** 135–149.

——, and F. C. Bosveld, 1997: Cabauw data for the validation of land surface parameterization schemes. *J. Climate,* **10,** 1172–1193.

Betts, A. K., J. H. Ball, and A. C. M. Beljaars, 1993: Comparison between the land surface response of the European Centre Model and the FIFE-1987 data. *Quart. J. Roy. Meteor. Soc.,* **119,** 975–1001.

Chen, F., K. Mitchell, J. Schaake, Y. Xue, H.-L. Pan, V. Koren, Q. Duan, and A. Betts, 1995: Modeling of land-surface evaporation by four schemes and comparison with FIFE observations. *J. Geophys. Res.,* **101,** 7251–7268.

Clapp, R. B., and G. M. Hornberger, 1978: Empirical equations for some soil hydraulic properties. *Water Resour. Res.,* **14,** 601–604.

Cosby, B. J., G. M. Hornberger, R. B. Clapp, and T. R. Ginn, 1984: A statistical exploration of the relationships of soil moisture characteristics to the physical properties of soils. *Water Resour. Res.,* **20,** 682–690.

Dickinson, R. E., A. Henderson-Sellers, P. J. Kennedy, and M. F. Wilson, 1986: Biosphere Atmosphere Transfer Scheme (BATS) for the NCAR Community Climate Model. NCAR Tech. Note TN275+STR, 69 pp. [Available from National Center for Atmospheric Research, P.O. Box 3000, Boulder, CO 80307.]

——, ——, and ——, 1993: Biosphere Atmosphere Transfer Scheme (BATS) Version 1e as coupled to the NCAR Community Climate Model. NCAR Tech. Note TN383+STR, 72 pp. [Available from National Center for Atmospheric Research, P.O. Box 3000, Boulder, CO 80307.]

Driedonks, A. G. M., H. van Dop, and H. Kohssied, 1978: Meteorological observations on the 213 m mast at Cabauw in the Netherlands. *Proc. Fourth Symp. Meteorological Observations and Instruments* Denver, CO, Amer. Meteor. Soc., 41–46.

Ducoudre, N. I., K. Laval, and A. Perrier, 1993: SECHIBA, a new set of parameterizations of the hydrologic exchanges at the land–atmosphere interface within the LMD atmospheric general circulation model. *J. Climate,* **6,** 248–273.

Dümenil, L., and E. Todini, 1992: A rainfall-runoff scheme for use in the Hamburg climate model. *Advances in Theoretical Hydrology,* J. P. O'Kane, Ed., European Geophysical Society Series on Hydrological Sciences, Vol. 1, Elsevier Science Publishers, 129–157.

Duynkerke, P. G., 1992: On the roughness length for heat and other vegetation parameters for a surface of short grass. *J. Appl. Meteor.,* **31,** 579–586.

Goutorbe, J. P., and C. Tarrieu, 1991: HAPEX-MOBILHY data base. *Land Surface Evaporation,* T. J. Schmugge and J. C. Andre, Eds., Springer-Verlag, 403–410.

Gregory, D., and R. N. B. Smith, 1994: Canopy, surface and soil hydrology. Unified Model Documentation Paper 25, 19 pp. [Available from U.K. Meteorological Office, London Road, Bracknell, Berkshire RG12 2SZ, United Kingdom.]

Henderson-Sellers, A., and V. B. Brown, 1992: Project for Intercomparison of Land Surface Parameterization Schemes (PILPS):

First science plan. GEWEX Tech. Note, IGPO Publ. Series 5, 53 pp.

——, A. J. Pitman, P. K. Love, P. Irannejad, and T. H. Chen, 1995: The Project for Intercomparison of Land-Surface Parameterization Schemes (PILPS): Phases 2 and 3. *Bull. Amer. Meteor. Soc.,* **76,** 489–503.

Holtslag, A. A. M., and A. P. van Ulden, 1983: A simple scheme for daytime estimates of the surface fluxes from routine weather data. *J. Climate Appl. Meteor.,* **22,** 517–529.

Kim, J., and M. Ek, 1995: A simulation of the surface energy budget and soil water content over the Hydrologic Atmospheric Pilot Experiments–Modelisation du Bilan Hydrique forest site. *J. Geophys. Res.,* **100,** 20 845–20 854.

Koster, R. D., and M. J. Suarez, 1992: Modelling the land surface boundary in climate models as a composite of independent vegetation stands. *J. Geophys. Res.,* **97,** 2697–2715.

Kowalczyk, E. A., J. R. Garratt, and P. B. Krummel, 1991: A soil-canopy scheme for use in a numerical model of the atmosphere—1D stand-alone model. CSIRO Division of Atmospheric Research Tech. Paper 23, 56 pp. [Available from CSIRO Division of Atmospheric Research, PMB 1, Aspendale, Vic. 3195, Australia.]

Liang, X., D. P. Lettenmaier, E. F. Wood, and S. J. Burges, 1994: A simple hydrologically based model of land surface water and energy fluxes for general circulation models. *J. Geophys. Res.,* **99** (D7), 415–428.

——, E. F. Wood, and D. P. Lettenmaier, 1996: Surface soil moisture parameterization of the VIC-2L model: Evaluation and modification. *Global Planet. Change,* **13,** 195–206.

Love, P. K., and A. Henderson-Sellers, 1995: Land surface climatologies of AMIP-PILPS models and identification of regions for future investigation (PILPS Phase 3a). GEWEX Tech. Note, IGPO Publ. Series 9, 47 pp.

Mahrt, L., and H.-L. Pan, 1984: A two-layer model of soil hydrology. *Bound.-Layer Meteor.,* **29,** 1–20.

Manabe, S., 1969: Climate and ocean circulation 1. The atmospheric circulation and the hydrology of the earth's surface. *Mon. Wea. Rev.,* **97,** 739–774.

Milly, P. C. D., 1994a: Climate, interseasonal storage of soil water, and the annual water balance. *Adv. Water Resour.,* **17,** 19–24.

——, 1994b: Climate, soil water storage, and the average annual water balance. *Water Resour. Res.,* **30,** 2143–2156.

——, R. D. Koster, and K. A. Dunne, 1995: Progress in phase 1(c) of the Project for Intercomparison of Land-Surface Parameterization Schemes (PILPS). *Extended Abstracts, Int. Union of Geodesy and Geophysics XXI General Assembly,* Boulder, CO, Amer. Geophys. Union, A 190.

Monna, W. A. A., and J. G. van der Vliet, 1987: Facilities for research and weather observations on the 213-m tower at Cabauw and at remote locations. Scientific Rep. WP-87-5, 27 pp.

Noilhan, J., and S. Planton, 1989: A simple parameterization of land surface processes for meteorological models. *Mon. Wea. Rev.,* **117,** 536–549.

Pan, H.-L., and L. Mahrt, 1987: Interaction between soil hydrology and boundary layer development. *Bound.-Layer Meteor.,* **38,** 185–202.

Pitman, A. J., and Coauthors, 1993: Results from the off-line control simulation phase of the Project for Intercomparison of Land-Surface Parameterization Schemes (PILPS). GEWEX Tech. Note, IGPO Publ. Series 7, 47 pp.

Polcher, J., K. Laval, L. Dümenil, J. Lean, and P. R. Rowntree, 1996: Comparing three land surface schemes used in GCM. *J. Hydrol.,* **180,** 373–394.

Robock, A., K. Ya. Vinnikov, C. A. Schlosser, N. A. Speranskaya, and Y. Xue, 1995: Use of midlatitude soil moisture and meteorological observations to validate soil moisture simulations with biosphere and bucket models. *J. Climate,* **8,** 15–35.

Rosenzweig, C., and F. Abramopoulos, 1997: Land-surface model development for the GISS GCM. *J. Climate,* in press.

Salvucci, G. D., and D. Entekhabi, 1994: Equivalent steady soil moisture profile and the time compression approximation in water balance modeling. *Water Resour. Res.,* **30,** 2737–2749.

Schaake, J. C., V. I. Koren, Q. Y. Duan, K. Mitchell, and F. Chen, 1995: A simple water balance model (SWB) for estimating runoff at different spatial and temporal scales. *J. Geophys. Res.,* **101,** 7461–7475.

Sellers, P. J., Y. Mintz, Y. C. Sud, and A. Dalcher, 1986: A Simple Biosphere Model (SiB) for use within general circulation models. *J. Atmos. Sci.,* **43,** 505–531.

Shao, Y., and Coauthors, 1994: Soil moisture simulation, a report of the RICE and PILPS workshop. GEWEX Tech. Note, IGPO Publ. Series 14, 179 pp.

Shmakin, A. B., A. Yu. Mikhailov, and S. A. Bulanov, 1993: Parameterization scheme of the land hydrology considering the orography at different spatial scales. *Exchange Processes at the Land Surface for a Range of Space and Time Scales,* H.-J. Bolle, R. A. Feddes, and J. D. Kalma, Eds., IAHS Press, 569–575.

Sutherland, R. A., 1986: Broadband and spectral emissivities (2–18 μm) of some natural soils and vegetation. *J. Atmos. Oceanic Technol.,* **3,** 199–202.

Verseghy, D. L., 1991: CLASS—A Canadian land surface scheme for GCMs. I. Soil model. *Int. J. Climatol.,* **11,** 111–133.

——, N. A. McFarlane, and M. Lazare, 1993: CLASS—A Canadian land surface scheme for GCMs. II. Vegetation model and coupled runs. *Int. J. Climatol.,* **13,** 347–370.

Warrilow, D. A., A. B. Sangster, and A. Slingo, 1986: Modelling of land surface processes and their influence on European climate. Dynamic Climatology Tech. Note 38, 94 pp. [Available from U.K. Meteorological Office, London Road, Bracknell, Berkshire RG12 2SZ, United Kingdom.]

Wetzel, P. J., and A. Boone, 1995: A Parameterization for Land–Atmosphere–Cloud Exchange (PLACE): Documentation and testing of a detailed process model of the partly cloudy boundary layer over heterogeneous land. *J. Climate,* **8,** 1810–1837.

Xue, Y., P. J. Sellers, J. L. Kinter, and J. Shukla, 1991: A simplified biosphere model for climate studies. *J. Climate,* **4,** 345–364.

Yang, Z.-L., R. E. Dickinson, A. Henderson-Sellers, and A. J. Pitman, 1995: Preliminary study of spin-up processes in land surface models with the first stage data of Project for Intercomparison of Land Surface Parameterization Schemes phase 1(a). *J. Geophys. Res.,* **100,** 16 553–16 578.